

A review on mechanical and metallurgical joining by plastic deformation

M. M. Kasaei¹ · R. Beygi¹ · R. J. C. Carbas¹ · E. A. S. Marques² · L. F. M. da Silva²

Received: 17 March 2023 / Accepted: 12 April 2023

Published online: 27 April 2023

© The Author(s) 2023 [OPEN](#)

Abstract

The substitution of traditional materials with lightweight materials in vehicle structures requires the development of new joining techniques which are capable of joining un-weldable alloys as well as dissimilar materials. Although conventional joining techniques such as fusion welding, adhesive bonding and mechanical fastening have matured in recent decades, their use for some of the above applications is limited. In this paper, recently developed joining techniques based on plastic deformation are presented and discussed. These techniques are divided into two categories, those based on mechanical interlocking and those based on metallurgical bonding. The first category covers clinching, self-pierce riveting and some innovative joining methods, and the second category covers friction stir welding and its variants. The focus of this study is on process development, process control and monitoring, process modelling, and joint characterization techniques. Finally, the two categories are compared, and their potential is discussed.

Keywords Joining by plastic deformation · Lightweight materials · Clinching · Self-piercing riveting · FSW · Novel joining processes

1 Introduction

Due to the increase of environmental pollution, as well as the reduction of fossil fuel resources, the automotive industry is under growing pressure to reduce the weight of vehicles while improving their efficiency [1]. This has become challenging since handling these issues should be accompanied by improving the comfort and safety of passengers. For this reason, a new concept for producing automotive body structures, called multi-material design, has been developed, in which each body part is made of a light material such as advanced high strength steel, aluminium and magnesium alloys, and composites according to the expected service requirements for the body structure [2]. This concept has been also accompanied by the increasing development of lightweight materials, but there is still a significant challenge associated to the manufacture of lightweight automotive structures, mainly due to difficulties in joining of dissimilar materials. Joining dissimilar materials using conventional methods like fusion welding is impossible or very difficult and inefficient due to differences in mechanical, physical and chemical properties. This has led to the development of joining processes based on plastic deformation. These processes can be divided into two categories: mechanical joining by plastic deformation and metallurgical joining by plastic deformation. In the first category, a form-fit and/or force-fit joint is created between the parts by applying plastic deformation, while in the second category, the connection is mainly

✉ R. Beygi, rbeygi@inegi.up.pt | ¹Institute of Science and Innovation in Mechanical and Industrial Engineering (INEGI), Rua Dr. Roberto Frias, 4200-465 Porto, Portugal. ²Departamento de Engenharia Mecânica, Faculdade de Engenharia, Universidade do Porto, Rua Dr. Roberto Frias, 4200-465 Porto, Portugal.



based on metallurgical bonding. Mechanical joining by plastic deformation such as clinching and self-piercing riveting have attracted much attention in recent years as it does not require fusion, allows for metallurgical bonding, and has high productivity and low energy consumption. New joining processes were also developed to meet existing needs for joining dissimilar materials in different shapes or different properties. In the mechanical joining by plastic deformation, the mechanical properties of the materials to be joined play an important role in the quality of the connection, and this should be taken into account to select and design an appropriate process.

In the second category, the friction welding, ultrasonic welding and friction stir welding (FSW) processes are used for metallurgical joining. In these processes, the metallurgical bond is formed by local plastic deformation, which primarily helps to disperse the barrier layer on the surfaces of the adjoining parts, such as the oxides. Secondly, the plastic deformation helps to bring the surfaces in each other's proximity in the atomic scale. Among these processes FSW has been intensively developed so that this process is now used in various applications such as space launch systems, automobiles, trains, airplanes, and even electronics [3]. The focus of this paper is therefore on FSW procedures due to their diversity and evolution over the past decades. Many industrial patents have been registered in transportation sector, especially in the automotive industry, however, the record of patents shows a declining trend indicating that this process has reached its maturity [4]. This process is widely used to join difficult-to-weld materials such as magnesium alloys [5] and aluminium alloys [6] which are categorized as light alloys. It is also used to join dissimilar materials which encounter serious problems when joined by common fusion welding processes [7]. In the case of dissimilar joining, mainly aluminium is involved to be joined to other materials like steel, copper, magnesium, and titanium. This process is based on a severe plastic deformation induced by a rotating tool. This plastic deformation causes a metallurgical bond to be established between the materials, though in some cases the mechanical interlocking may accompany the metallurgical bonding like self-riveting FSW [8]. In some cases, this process is used to establish only the mechanical interlocking without any metallurgical bonding like friction stir extrusion developed by Evans et al. [9]. The contribution of mechanical interlocking in the case of dissimilar welding is more significant than similar welding. This is because the metallurgical bonding is associated with intermetallic formation which is brittle and can degrade the bond strength when the thickness exceeds a critical value.

As industrial examples, FSW is used to fabricate large volume fuel tanks made of AA2219 which are used in the launch vehicles used in the aerospace industry (Fig. 1) [10]. It is also used by Honda, to produce hybrid structure of aluminium-steel used in the sub frame of one of its automobiles leading to a 25% reduction in weight (Fig. 2) [11].

The two categories of joining by plastic deformation, mechanical and metallurgical, have been reviewed separately in various literatures. Though the mechanism of joining in these two processes are different, they have potential to be interchangeably used for joining some lightweight materials. There is a lack of literature to compare these processes together. In this paper, the most important developments in mechanical and metallurgical joining processes by plastic deformation including clinching, self-piercing riveting, innovative technologies and FSW are explored. The focus is on

Fig. 1 Structure and main welds of a launch vehicle tank [10]. (Reprinted with permission from Elsevier)

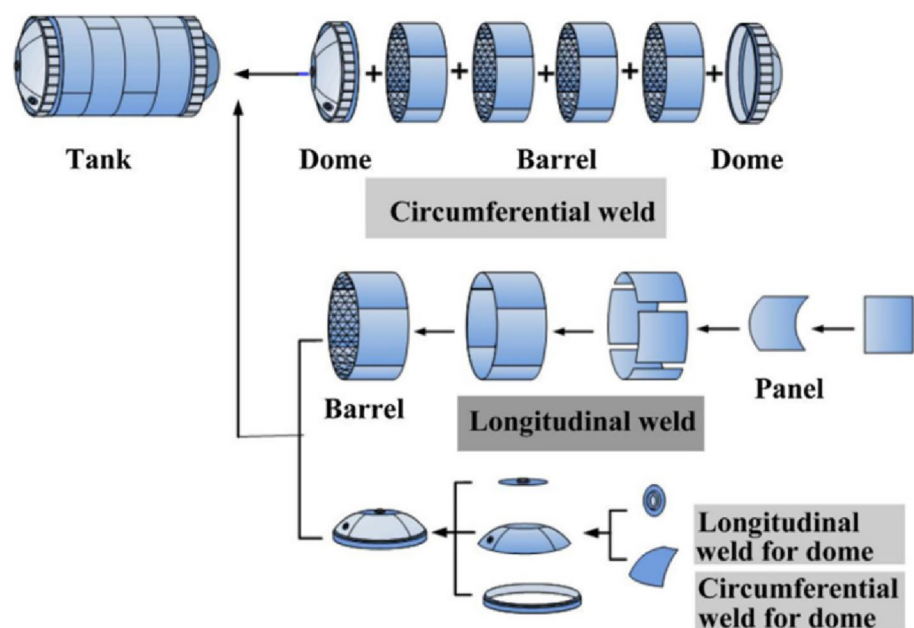
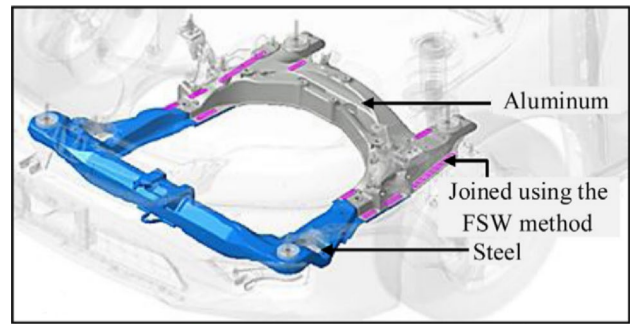


Fig. 2 A subframe of a Honda car made of aluminium-steel hybrid structure joined by FSW [11]. (Reprinted with permission from Elsevier)



process development, process control and monitoring, process modelling, and joint characterization techniques. Finally, the two categories are compared, and their potential are discovered.

2 Mechanical joining by plastic deformation

2.1 Process development

2.1.1 Clinching

Clinching is a highly productive and cost-efficient joining process based on plastic deformation that can be used to attach sheet parts without auxiliary elements. In this process, as shown in Fig. 3, the tool components include a punch, a die, and a blank holder. After being fixed on the die by the blank holder, the sheets are locally and severely deformed by the punch and inserted into the die cavity. Spreading the sheets inside the die cavity leads to a form-fit and force fit joint. The main characteristics of a clinched joint that affects the mechanical properties of the joint are neck thickness, interlock, diameter and bottom thickness [12].

The clinching process has been utilized to connect a wide variety of similar or dissimilar materials, including steel, aluminium, copper and titanium alloys, polymers and composites. However, historically there have been important limitations for joining sheets with high strength or low ductility, which have led to changes in the tool design or the development of new variant of this process. One of these variants is hole clinching, in which a sheet with low ductility is punched or drilled and then placed on the die side, while the deformable sheet is placed on the punch side and formed inside the hole of the die-sided sheet and the cavity of the die (see Fig. 4a).

Lee et al. [13] presented the relationships among shear strength, tool geometry and mechanical interlock shape in the hole clinching. A design procedure, proposed by combining these relationships and the finite element analysis was used to join Al6061-T4 alloy to dual phase steel, hot-pressed steel, and carbon-fibre-reinforced polymers (CFRP). The manufactured joints satisfied the design requirements by withstanding shear fracture loads of more than 2.5 kN and failing in a neck fracture mode. However, this process faces serious challenges when the punch-sided sheet has a higher strength compared to the die-sided sheet. In addition, the delamination of the CFRP sheet can be expected in the hole edge due to the metal flow [14]. To decrease the damage of the CFRP sheet and increase the formability of the punch-sided sheet,

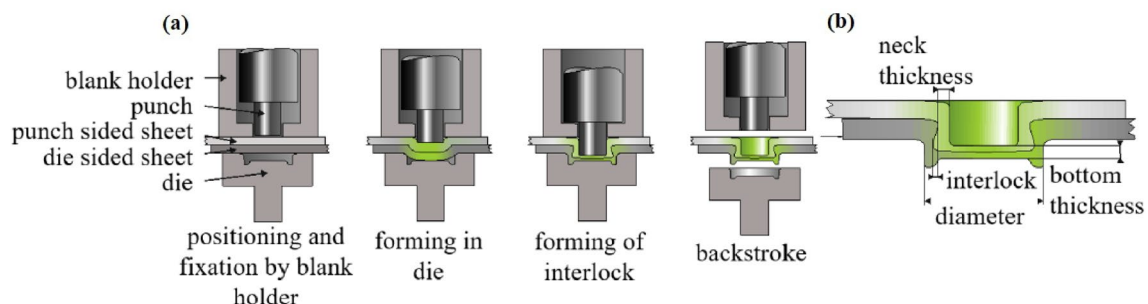


Fig. 3 Schematic representation of the clinching process: **a** the clinching stages, and **b** the main characteristics of a clinched joint [12]. (Reprinted with permission from Elsevier)

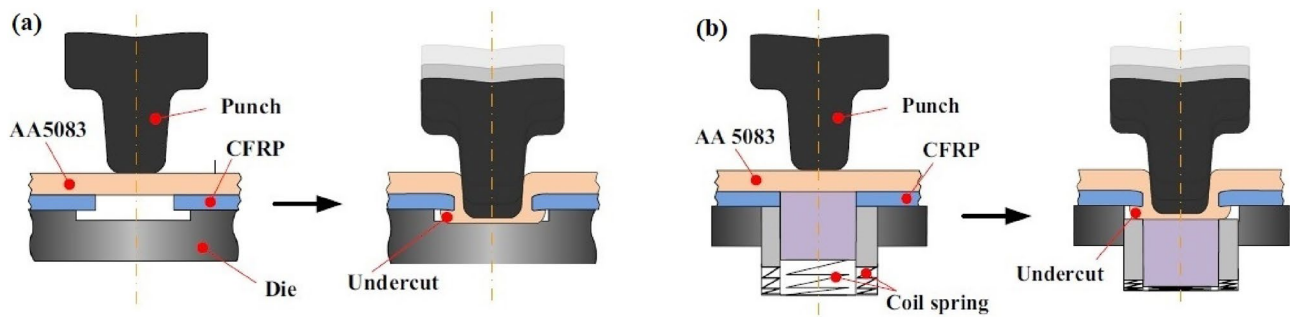


Fig. 4 Schematic representation of the hole clinching process with **a** a conventional die, and **b** a spring die [15]. (Reprinted with permission from Elsevier)

a spring die was proposed for the hole clinching in which two pads supported by a coil spring are employed to enhance the hydrostatic pressure during the deformation (see Fig. 4b) [15]. It was reported that this technique can reduce about 50% damage to the neck region of the punch-sided sheet and prevent defects, like neck fracture and damage to CFRP, leading to a button separation mode in the single lap shear test.

To decrease operation times and increase productivity, the punching and clinching stages were combined in a single-stage process called shear clinching [16]. In this process, as shown in Fig. 5, with the movement of the punch, first the die-sided sheet is cut by the sharp edge of the die, and then the punch-sided sheet, which must have sufficient ductility, is deformed inside the hole and the die cavity. Like hole clinching, shear clinching can be employed for joining ultra-high strength steels (UHSS) and aluminium alloys, but two necks formed in the punch-sided sheet lead to a lower strength [17]. Both the shear and hole clinching processes are restricted by the mechanical properties of the punch-sided sheet due to severe deformation. For instance, the shear-clinching of AA7075-T6 which is a high-strength aluminium alloy with low ductility, is not applicable [18]. It was reported that a short-term heat treatment by a laser can be efficient on the improvement of the joinability of this alloy. The shear clinching was also examined for attaching three sheets made from AA5182-O and DP600 with different configurations [19]. It was revealed that although under shear load, the strength of the three-sheet joint is similar to the two-sheet joint, applying tensile load results to a two-staged failure mode and thus to lower strength.

The use of heat has been a suitable solution for connecting polymers and composites to the metallic sheets in the clinching process. Lambiase [20] heated different thermoplastic polymers (PS, PC and PMMA) by a convective source and joined successfully them as the die-sided sheet to aluminium sheets as the punch-sided sheet. Nevertheless, a hole was observed in the polymer sheet, which can affect the quality of the clinched joint. Krassmann and Moritzer [21] formed thermomechanically a thermoplastic composite to reduce damage to glass fibres during the formation of the mechanical interlock in the hole clinching process. The created joints showed lower strengths by changing the loading direction from shear to cross-tension in the quasi-static destructive tests. Despite the efforts that have been made in adapting the clinching process for creating hybrid metal-composite/polymer joints, this process still needs further development to be used in industrial applications.

In recent years, flat clinching and dieless clinching processes have been proposed since they can make one-sided flat joints due to the use of a flat anvil instead of a groove die (Fig. 6) [22]. This feature can increase the applications of clinched joints both functionally and aesthetically. In the dieless clinching, a shouldered punch is used which means that unlike the flat clinching process, there is no need a blank holder [23]. These processes make the adjustment between the punch and the die easier. However, they require more force to produce joints compared to the conventional clinching

Fig. 5 Schematic representation of the shear clinching process [19]. (Reprinted with permission from Elsevier)

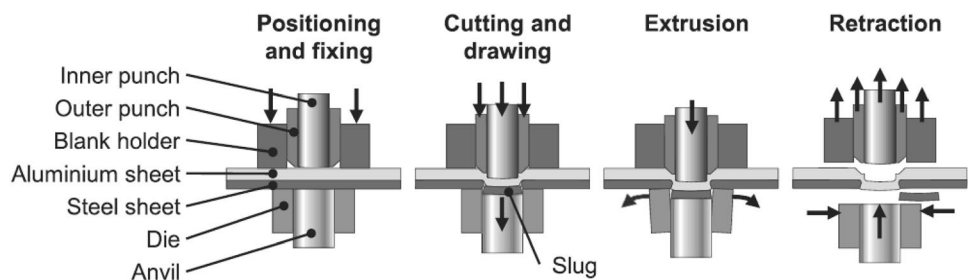
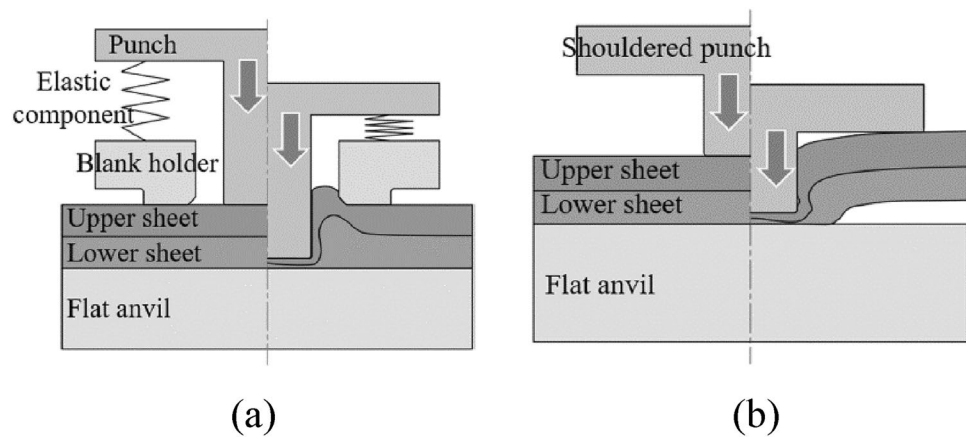


Fig. 6 Schematic representation of **a** the flat clinching and **b** the dieless clinching [22]. (Reprinted with permission from Elsevier)



process. In the design of dieless clinched joints for dissimilar aluminium alloys, it is worth mentioning that as the upper sheet has a higher strength, the joint shows better mechanical behaviour [23]. In the heat assisted clinching, the flat anvil improves the heat transfer from the die to the die-sided sheet. The hot die-less clinching process was successfully tested for high strength AA7075-T6 sheets [24] as well as low ductility magnesium sheets [25].

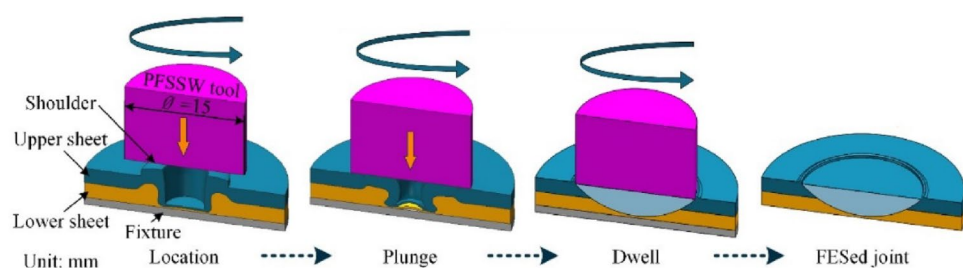
Friedrich et al. [26] added a deformable auxiliary element in a second forming stage to the flat clinched joints to increase the interlocking leading to an improvement in the joint strength. A rigid auxiliary element was also employed to enhance the strength of flat-clinched joints [27]. In this process, called rivet clinching, a cylindrical rivet is pressed into the sheets by applying an external force to form a mechanical interlock. One of the key parameters in this process is the blank holder force so that increasing it allows to avoid warping and bulging of the joints and increase the tensile and shear strength [28]. It should be noted that the addition of an auxiliary element increases the joint weight and cost.

In order to manufacture clinched joints with double-sided flat surfaces, the initial dieless clinched joints can be flattened by a pair of flat dies in a second forming stage [29, 30]. These joints are suitable for functional surfaces. As shown in Fig. 7, friction stir spot welding was also proposed to repair the hole of the flat clinched joints and improve the mechanical behaviour [31]. In this method, the protruding material on the punch-sided surface is forced into the hole under frictional heat and forming force. It was reported that the strength of the repaired joints between two similar aluminium sheets is significantly higher than that of flat-clinched joints because of the formation of metallurgical bonding. However, in case of dissimilar materials, involving heat may cause the formation of a brittle intermetallic compound layer affecting joint properties. Furthermore, the increase of the process time and cost should be taken into account.

Laser shock flat hole clinching process can be used to create microscale joints between ductile and brittle materials [32]. In this process, a ductile metal foil is plastically formed by laser-induced shock wave into the hole of a pre-pierced foil [33]. This process was successfully tested for joining pure copper and stainless-steel foils. However, the pulsed laser energy, number of laser pulses, and laser spot diameter should be carefully determined to obtain a sound joint [34].

Adhesive bonding can be combined with the clinching process to provide a higher shear strength, better fatigue performance, vibration absorption and corrosion resistance for structural joints (Fig. 8) [35]. Nevertheless, the adhesive has a negligible effect on the performance of the clinch-bonded joint under tensile load because of the low tensile strength of the adhesive [36]. In this hybrid process, an adhesive is first added between the joining partners and the clinching operation is then performed when the adhesive is still fluid. The final strength of the hybrid joint is attained after the adhesive is entirely cured. During the clinching process, adhesive flow can cause the formation of adhesive pockets near

Fig. 7 Schematic representation of refilling the keyhole of a flat-clinched joint by friction stir spot welding [31]. (Reprinted with permission from Elsevier)



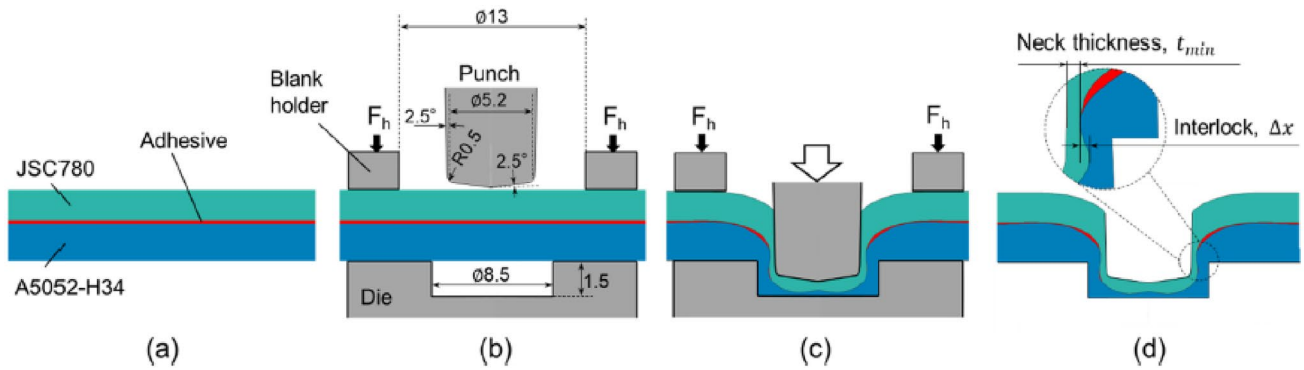


Fig. 8 Schematic representation of the clinch-bonding process designed for joining aluminium alloy AA5052-H34 and advanced high-strength steel JSC780: **a** adhesive injection, **b** clamping, **c** clinching, and **d** tool releasing (unit: mm) [26]. (Reprinted with permission from Elsevier)

the joint which negatively influences the creation of mechanical interlock and, therefore, the mechanical properties of the joint [37]. The combination of the adhesive bonding and clinching processes was also tested in microscale where an adhesive was placed between two aluminium foils and then attached to a pre-drilled thin stainless-steel sheet by laser shock [38]. This process, called laser shock adhesive-clinching, can create a hybrid joint with a higher shear strength compared to the pure bonded and the pure clinched joints. It worth mentioning that the addition of an adhesive increases the sensitivity of the connection to environmental conditions, including temperature and humidity.

2.1.2 Self-piercing riveting

Self-piercing riveting (SPR) is another joining process where an auxiliary joining element is used. In this process two or more sheets are joined by driving a rivet that pierces the upper sheet and flares within the lower sheet to form a force-fit and form-fit joint [39]. In this process, a pre-drilled hole is not required unlike the conventional riveting, decreasing the processing time [40, 41]. Figure 9 shows the four stages of the process. In the SPR process, four components, including a die, a punch, a blank holder and a consumable rivet are needed. The process starts by lowering the blank holder and clamping the sheets on the die. The punch is then moved down to force the rivet into the sheets by either punching or pushing until it starts to flare and form a mechanical interlock. Finally, the punch is retracted, and the joined sheets are released from the die. Interlock, minimum die-sided material thickness and rivet head end position are most important geometrical characteristics of a SPR joint that influence its load bearing capacity.

Self-piercing riveting can be used to connect a wide range of materials, including dissimilar lightweight materials such as aluminium to advanced high strength steel, aluminium to magnesium alloy and aluminium alloys to composite. Compared to clinching, this process is less sensitive to material formability, allowing to expand its applications in the manufacturing of multi-material automotive bodies, however, when the strengths of the joining partners are very different, self-piercing riveting becomes challenging [42]. In the joining of advanced high strength steel and aluminium alloys,

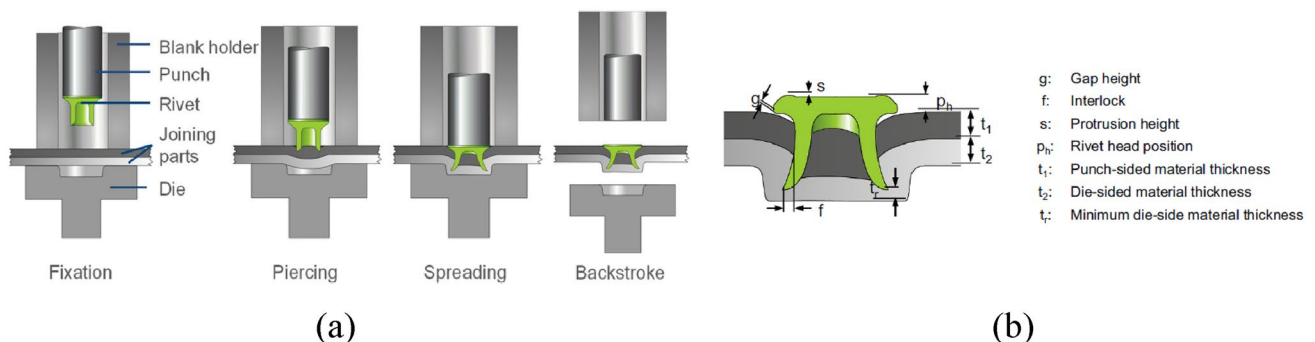


Fig. 9 Schematic representation of the self-piercing riveting (SPR) process **a** the process stages **a**, and **b** the characteristics of a SPR joint [41]. (Reprinted with permission from Elsevier)

it becomes difficult to insert the rivet into the high strength steel sheet on the upper side. Furthermore, placing the high strength sheet on the lower side may cause insufficient flare of the rivet skirt or even the occurrence of fracture in this sheet [43]. The optimization of the shape of the die can help to increase the joinability of such material combinations [44]. The use of innovative materials like high nitrogen steel, which has a high strength along with a good ductility and corrosion resistance, in the manufacturing of rivets can be an alternative solution to join high-strength materials. In this regard, Kuball et al. [45] presented a two-stage forming process for the manufacture of high nitrogen steel rivets, which can also eliminate the secondary processes of heat treatment and coating in the manufacture of rivets.

Friction self-piercing riveting (F-SPR) combines self-piercing riveting and friction stir welding to join lightweight materials with low formability and high strength without cracking, particularly in cases of joining aluminium and magnesium alloys (see Fig. 10). In this process, a rivet is inserted into the sheets while being rotated by a spindle. The sheets are softened by the frictional heat generated by the rivet rotation, leading to higher formability for materials and lower force for feeding the rivet. In addition to the formation of a mechanical interlocking by flaring the rivet, the frictional heat can also create metallurgical bonding between the sheets resulting in improved joint strength [46].

Ma et al. [47] employed the F-SPR process to connect high strength AA7075-T6 aluminium sheets and investigated influence of the spindle speed and rivet feed rate on joint characteristics, joining force and energy input during the process. It was revealed that the combination of a medium rivet feed rate of 3–5 mm/s and a high spindle speed of 3000 rpm results in joints with the highest quality. In addition, the shear strength of the F-SPR joints was the 67.6% and 13.9% higher than the SPR and friction stir spot welded joints, respectively. However, the energy consumption in the F-SPR process should be taken into account because 96% of the total energy is used for the spinning motion [47]. The SPR and F-SPR were also examined to join AA6061-T6 aluminium alloy and AZ31B magnesium alloy. It was reported that that better joint quality can be achieved in both the processes by riveting from the magnesium sheet to the aluminium sheet. Furthermore, in the F-SPR process, the force required for riveting decreases to one third of that in the SPR process while the shear strength of the F-SPR joints increases 45.4% due to better rivet flaring. Shan et al. [48] proposed the friction stir riveting (FSR) process to join aluminium alloy and advanced high strength steel sheets. In this process, after piercing the aluminium sheet, a rotating rivet is frictionally welded to the steel sheet to create a metallurgical-mechanical hybrid joint. In fact, in the FSR process, the rivet does not pierce the steel sheet that allows to expand the applications to wider material combinations compared to the F-SPR process. However, the performance of FSR joints is negatively affected by a thin inclusion layer in the welding zone.

Injection lap riveting was proposed to eliminate the penetration of the sheets by a rivet, which limits the application of the FSR process for materials with high strength or low ductility [49]. In this process, as shown in Fig. 11, the desired shape of a semi-tubular in a riveted joint is first machined in the joining partners and afterwards the rivet is injected through the machined holes to achieve the interlocking. This design allows the rivets to be made of the materials of the sheets. This process was successfully tested for joining hybrid busbars, electric conductive connections, made from copper and aluminium using a copper rivet to reduce the electrical disruption. The resulting joints do not have protrusions above and below the sheet surfaces resulting more uniform the electric current flow.

The self-pierce riveting process is a very rigid and inflexible process as it has few controllable parameters to adapt to different conditions. The addition of a tumbling punch to the conventional self-pierce riveting process can create

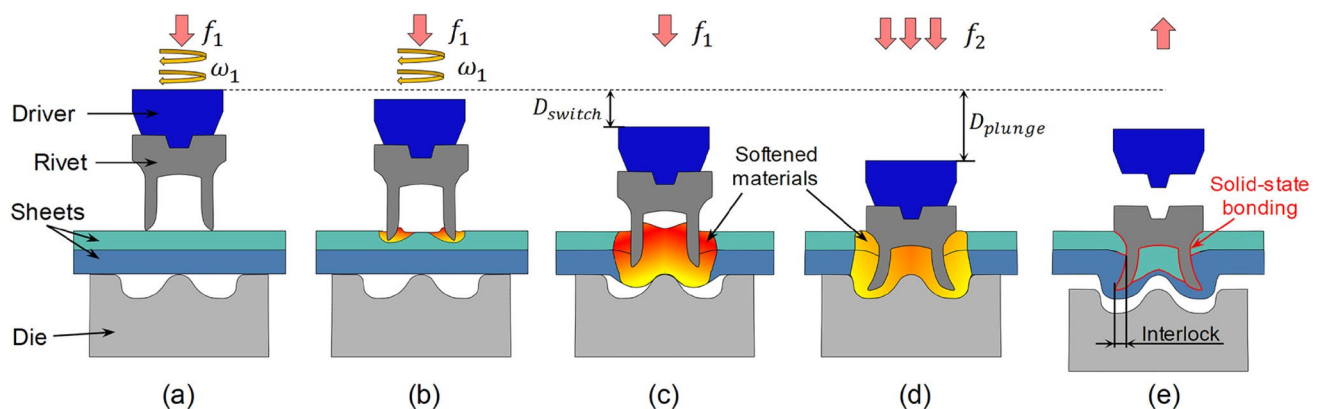
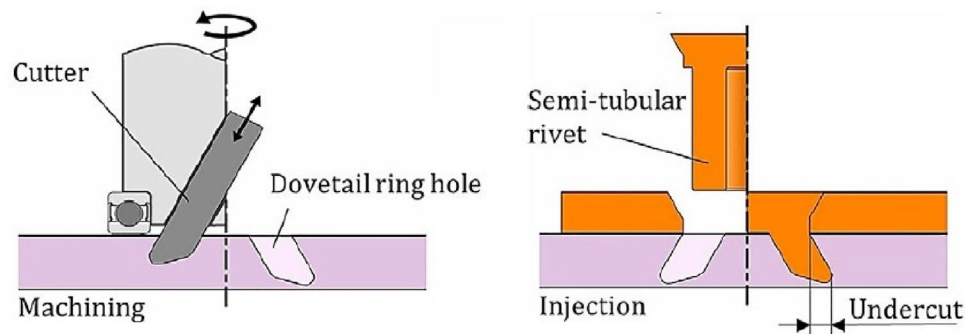


Fig. 10 Schematic representation of the friction self-piercing riveting (F-SPR): **a** positioning, **b** friction softening, **c** quick stop, **d** riveting **e** tool releasing [46]. (Reprinted with permission from Elsevier)

Fig. 11 Schematic representation of the injection lap riveting process [49]. (Reprinted with permission from Elsevier)

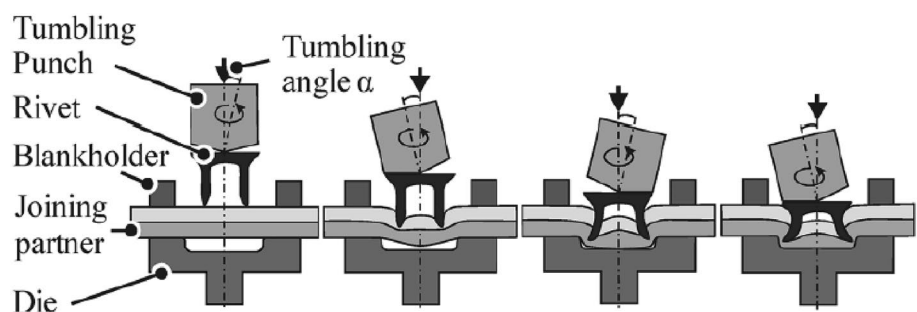


possibilities for a versatile joining process as shown in Fig. 12 [50]. The tumbling motion of the punch reduces the contact area between the punch, which has a conical geometry, and the rivet. As a result of this, the contact pressure for a constant force increases, leading to the improvement of material flow and forming capacity. Wituschek and Lechner [50] tested different tumbling angles for joining similar aluminium sheets and found that the joining force decreases with the increase of the tumbling angle up to 31%. The selection of circular or spiral tumbling kinematics for the punch can affect both the characteristics of mono- and multi-material joints and the force required for the joining process [51]. However, the tumbling onset influences slightly the geometric characteristics of the joint, but has a significant effect on the evolution the joining force with the punch displacement [50]. The increase of the tumbling punch speed creates a more uniform deformation of the rivet head and decreases the joining force. Wituschek et al. [52] showed that the tumbling self-piercing riveted joints, compared to the conventional self-piercing riveted joints made between a dual-phase steel and an aluminium alloy, withstand a higher force in the shear tests and have a significantly higher energy absorption in cross tensile tests.

The geometry of the rivet can be varied to adapt the process for different purposes. Kato et al. [53] developed a short thin pipe rivet in a process called double-sided self-pierce riveting (DSSPR). The pipe rivet, with chamfered ends, is placed between the sheets and with a single stroke the rivet pierces and holds the sheets together. Nonetheless, the conventional DSSPR process has limitations when joining dissimilar materials with very different strengths, as the rivet is less pierced in the sheet with higher strength resulting in an asymmetrical mechanical interlock. Alves et al. [54] studied the joining of AA5754-H111 and PVC by the DSSPR process using rivets with different chamfered angles in each side and also by a two-stroke approach where the higher strength material is firstly pierced by the rivet and only then the PVC sheet is placed for the second stroke. In another study, Alves et al. [55] studied the feasibility of introducing a flat-bottom hole in the sheet with higher strength in which the rivet, with different chamfered angles, can be inserted. With this method, the positioning and alignment of the rivets was solved and the joint strength was also considerably improved when compared with a conventional DSSPR joint.

The SPR process is adopted to join CFRP laminates to lightweight metals, especially aluminium alloys, for the construction of multi-material hybrid body structures [56]. Since this technique can be employed only when the material placed on the bottom side has sufficient ductility, CFRP composites are often considered as the top sheet and the metal sheets undergo severe deformation during SPR process. Mechanical properties of the hybrid joints are influenced by geometrical features and process parameters such as rivet shape and riveting force. When continuous fibres are adopted as reinforcement, the fibre fractures, matrix cracks, and delamination are often present near the joint [57]. To decrease

Fig. 12 Schematic representation of the self-pierce riveting process combined with a tumbling punch [51]. (Reprinted with permission from Springer)



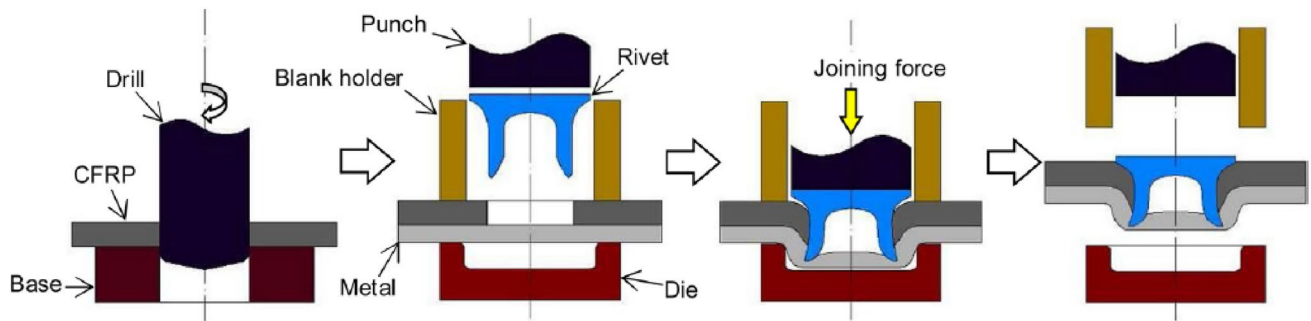


Fig. 13 Schematic representation of the pre-holed self-piercing riveting process for creating CFRP-metal joints [59]. (Reprinted with permission from Elsevier)

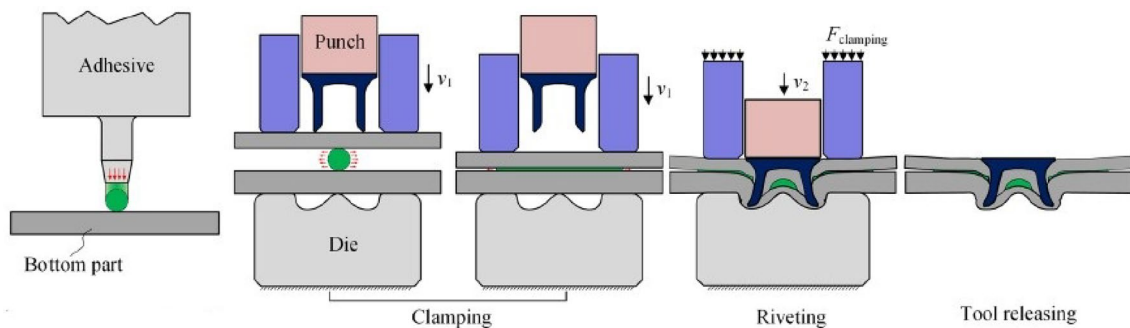


Fig. 14 Schematic representation of the stages of the self-pierce riveting-bonding process [62]. (Reprinted with permission from Elsevier)

these defects, Wang et al. [58] proposed a post-curing self-piercing riveting (PC-SPR) technique in which the CFRP sheet are cured after the performance of the joining process.

In the conventional SPR method, the broken fibres usually exist at the region below the rivet tail. Zhang et al. [59] applied a pre-holed self-piercing riveting (PH-SPR) method to remove this defect and also obtain a better mechanical interlock in the riveted joints between CFRP and pure titanium sheets (see Fig. 13). In this process, the CFRP sheet is drilled before the joining process and, therefore, the rivet tail enters directly into the contact with the metal sheet resulting in a tighter mechanical interlock. Rao et al. [60] proposed new die and rivet geometries to join discontinuous carbon fibre reinforced thermoplastic composites. In this design, the rivet skirt pierces thoroughly both upper and lower sheets and flares along the trough surfaces of the die to form a mechanical hook. Vorderbrüggen and Meschut [61] investigated the damage to self-piercing riveted CFRP-metal joints due to the heat generated in the paint shop of an automotive body and optimized the geometry of rivet to ensure the requirements of the automotive industry.

SPR and bonding processes are combined to share their advantages and cover each other's limitations (refer to Fig. 14) [62]. The adhesive layer reduces the corrosion between dissimilar materials [63] and also reduces the stress concentration in the SPR joint and can lead to an increase in its static and fatigue strengths under shear loading condition [64]. Unlike bonded joints, hybrid bonded-SPR joints are less sensitive to environmental conditions [64]. Yang et al. [65] investigated the influence of adhesive introduction on F-SPR method for the joining of AA7075-T6 aluminium sheets. The adhesive reduced the mechanical interlock by decreasing the contact stiffness and the friction coefficient between the aluminium sheets but did not influence the metallurgical bonding between the joining partners. Although the cured adhesive had no clear effect on the joint strength in the cross-tension test, enhanced the shear strength and energy absorption of the hybrid joint in the shear test by 128.7% and 82.5% respectively.

Liu and Zhuang [66] proposed $0^\circ/90^\circ$ ply of CFRP to obtain the optimum mechanical performance for the SPR-bonded joints of CFRP and AA5754 aluminium sheets under shear loading condition. The adhesive and locked structure failure mode was observed in these hybrid joints. Jiang et al. [67] applied SPR-bonding hybrid method to join aluminium and steel sheets and found that the hybrid joint provides 177.3% greater shear strength than that of the SPR joint and 360.0% and 47.9% higher energy absorption compared to the SPR and adhesive bonded joint, respectively. In fact, the mechanical interlock does not play a role in the load bearing capacity of the hybrid joint in the shear test until the adhesive failure,

and after that it prevents the sudden drop in load and, therefore, improves reliability of the joint. The above-mentioned studies allow to conclude that the combination of adhesive bonding and joining by plastic deformation can provide the joints with great mechanical properties.

2.1.3 Novel joining processes

Innovative processes have been developed to join materials with different shapes or properties, or for specific applications, in which common joining methods by plastic deformation are not applicable or efficient. Connecting tubes to sheets is one of these challenging issues. Alves et al. [68] developed an innovative joining method based on plastic instability to connect thin-walled tubes to sheets made of dissimilar materials. In this joining method, an axial compression force is applied to a tube to initiate local buckling, resulting in the development of plastic waves. The plastic waves are then controlled and converted into compression beads. Two compression beads are required to connect a tube to a sheet (Fig. 15a) unless one compression bead is combined with forms created by other deformations like sheet-bulk forming or flaring (Fig. 15b) [69, 70]. The method was also applied for joining thin-walled tubes from their ends [71]. Alves et al. [72] used the idea of the self-pierce riveting to join tubes to sheets. In this technique, a tube with the sharpened end is pressed into the sheet to form a mechanical lock (Fig. 15c). Afonso et al. [73] proposed a two-stage operation based on the combination of boss forming and upsetting to join tubes to sheets. First, an annular flange around a tube is formed by partial compression of the tube wall thickness along the tube axis (boss forming), and then this flange is compressed against a sheet with a bevelled hole (upsetting).

Creating connections for specific applications like the joining of hybrid busbars in electric vehicles, has been another motivation for developing new processes. A new method for joining by plastic deformation without auxiliary elements was developed by combining cutting, bending and compression operations for the fabrication of strong lap joints in hybrid busbars made from thick copper and aluminium strips [74, 75]. Sampaio et al. [76] proposed a new self-clinching fastening process involve making a blind hole in each sheet and locating a special designed fastener with the annular groove in the holes of the sheets. A hidden lap joint is then created by pressing the sheets against each other to form material around the fastener into the annular grooves (Fig. 16). The process was also tested to manufacture busbars [77].

Newly, a novel joining process, termed 'hole hemming', has been developed by Kasaei and da Silva [78] for connecting two sheets made from dissimilar materials in which only one of the sheets should be sufficiently ductile, and the strength and ductility of the second sheet does not limit the joining process (refer to Fig. 17). Thus, the second sheet can be a polymer, composite, low-ductility or high-strength metal. The hole hemming process involves in creating a mechanical interlock between predrilled holes that can be produced anywhere on the sheets. The process is performed in a two-stage operation including flanging the hole of an outer sheet and bending the flange over the hole of an inner sheet. The process can realize joining materials with very different mechanical properties without heating or using additional elements such as a rivet.

Despite the innovative processes developed, the connection of metallic materials to composites and polymers still remain as a serious challenge. According to the features of the hole hemming, this process can be a promising solution

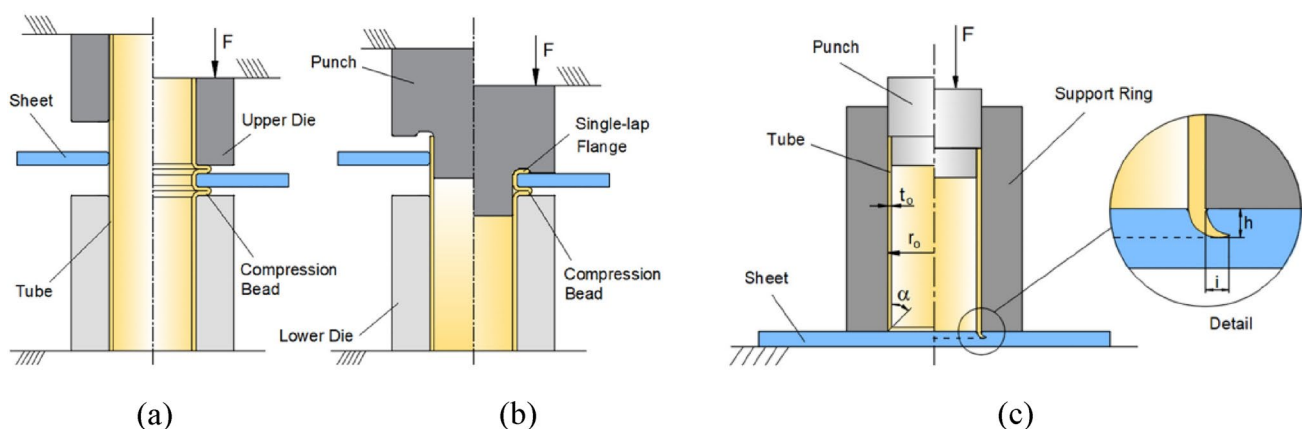


Fig. 15 Joining tubes to sheets by **a** plastic instability **b** by the plastic instability and flaring and **c** self-pierce riveting [16]. (Reprinted with permission from Elsevier)

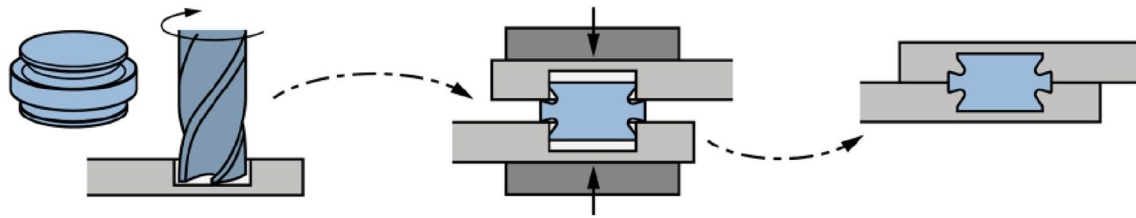


Fig. 16 Schematic representation of the self-clinching fastening process [76]. (Reprinted with permission from Elsevier)

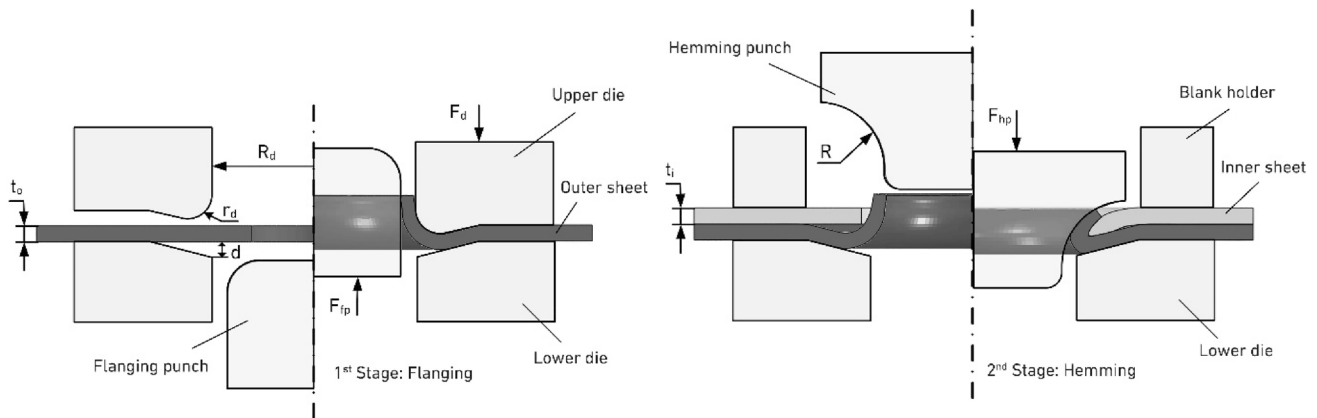


Fig. 17 Schematic representation of the hole hemming process

for this kind of the connections. However, in applications where sealing is important, the use of the hole-hemmed joints is limited. Since the use of products produced by additive manufacturing has continuously increased, it is necessary to develop their appropriate connection methods that would be an interesting issue for future work.

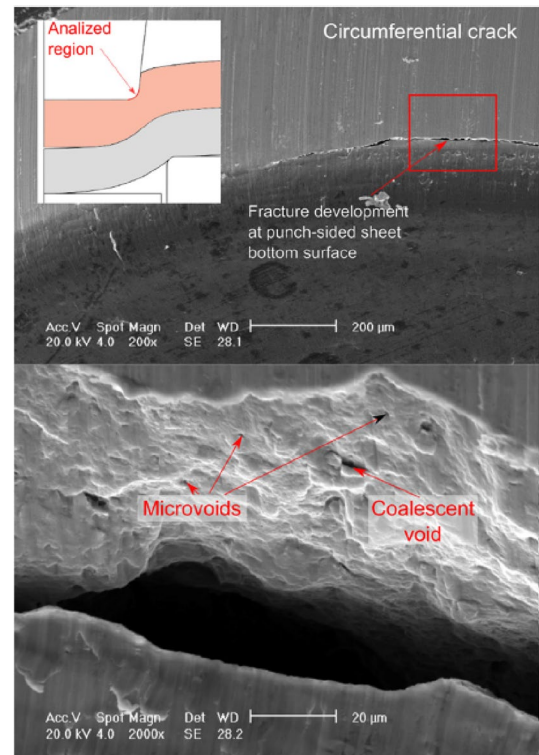
2.2 Joint evaluation

To evaluate the quality of the mechanical interlock produced by plastic deformation, the cross-section of joints is commonly analysed. To this end, the joints are cut in the middle and the resulting cross-sections are then examined by means of an optical microscope [29]. The main geometrical characteristics of the joints are measured from cross-sectional micrographs. In the case of composites, structure degradation in polymer and fibre damage are also evaluated [58, 59]. Fractography is performed by scanning electron microscopy (SEM) to identify the origins of fracture in joining partners [79] (Fig. 18). In addition, the effect of severe local deformations on the parts to be joined can be investigated by examining their grain structures and hardness before and after the plastic deformation [80, 81]. It is expected that grain orientations and hardness are changed in different parts of the joint which are non-uniformly work-hardened.

The joints created by mechanical joining processes by plastic deformation are examined by means of destructive tests such as single-lap shear, cross-tension and peel tests to determine the maximum forces that the joints can safely resist and their failure modes [22, 82]. In addition, the relationships among the process parameters, the joint characteristics and the joint strength are explored. The joints are also tested under impact and cyclic loading conditions to investigate the safety and durability of the structure [64, 83]. Different load levels are used for these tests. A high-speed camera can be used to identify the crack propagation process and its path. Experimental data is correlated with the numerical results of the static, impact and fatigue responses of the joints.

Although the performance of joints under static loading has been widely investigated and their failure mechanisms have been determined, the study of the performance of the joints under impact and cyclic loads needs further investigation. This is due to the fact that these joints have been mostly developed for the construction of automotive structures, where the tolerance of these types of loads is of great importance. In addition, it seems necessary to develop new tests that allow checking the mechanical properties of the joints under mix loads such as a shear-tensile load which are likely to exist in the structures.

Fig. 18 The surface morphology of upper surface of punch-sided sheet during the clinching process of AA6082-T6 sheets [79]. (Reprinted with permission from Elsevier)



2.3 Fracture modelling

The finite element method has been extensively employed to simulate the mechanical joining processes by plastic deformation [84, 85]. Finite element simulations are mostly used to understand the effects of process parameters and tool geometry on joint characteristics, to optimize them to obtain a better mechanical interlock, and to predict the required force during a joining process. Destructive tests are also modelled to predict the strength and failure mode of joints under different loading conditions. The most important limiting factor for joining processes based on plastic deformation is the formability of materials, which is limited by fracture. Thus, considering fracture criteria in the finite element analysis of these processes can help to increase the accuracy of predictions [86]. However, this has been ignored in most of the investigations to simplify the modelling procedure. Defining the fracture behaviour of materials in the finite element model of the SPR process, in which the upper sheet is cut by a rivet, is essential. For this reason, the finite element method has been used less in the SPR process compared to the clinching process, and most of the investigations is based on experimental tests, which increases significantly research cost [47, 51]. In addition, when one of joining partners is made of composites, experimental testing is usually preferred due to the difficulties of modelling their deformation behaviour and failure [58].

Lambiase and Ilio [79] employed the Rice and Tracey criterion to model ductile damage during the clinching process of AA6082-T6 sheets and introduced the punch-sided sheet neck and die-sided sheet bulge as the critical regions. Wiesenmayer and Merklein [18, 19] modelled the cutting of the die-sided sheet in the shear clinching process by the Cockcroft-Latham criterion. Lee et al. [15] established the process windows of the hole clinching for the joining of CFRP and AA5083 aluminium alloy sheets using the normalized Cockcroft-Latham criterion. Liu et al. [14] investigated the influence of ply angle on the damage pattern in the CFRP laminate by means of a continuous damage model based on the modified Hashin failure criterion during the hole clinching of CFRP and aluminium sheets.

Karathanasopoulos et al. [87] explored the SPR of different aluminium alloy and dual-phase steel sheets in terms of the rivet and die geometries using finite element and neural network modelling. The authors used the Hosford-Coulomb fracture criterion calibrated under different loading conditions to model the penetrations of the rivet into the sheets (refer to Fig. 19). In another investigation, they modelled failure mechanisms of the SPR joint in the lap-shear, cross-tension, inclined cross tension and peel tests [88].

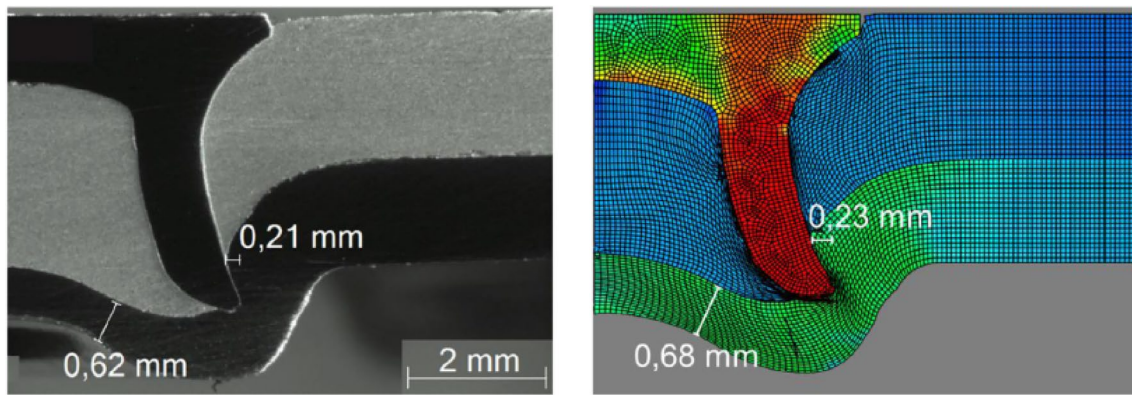
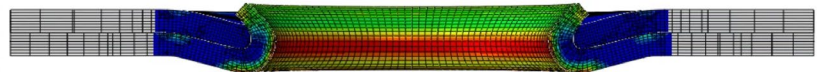
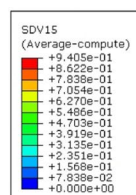


Fig. 19 Comparison of the cross-section of the SPR joint obtained from the experimental test and the numerical simulation considering the Hosford-Coulomb fracture criterion. (materials: 2.1 mm AA7075-F/1.5 mm DP600 steel) [87]. (Reprinted with permission from Elsevier)

Fig. 20 Damage distribution in the hole hemmed joint predicted based on the Modified Mohr–Coulomb criterion (materials: 1 mm DP780 steel/1 mm AA6061-T6 steel)



Kasaei and da Silva [78] developed the hole hemming process for joining a dual phase steel, DP780, and an aluminium alloy, AA6061-T6, by finite element modelling. They predicted the damage evolution based the Modified Mohr–Coulomb criterion during the hole hemming process (see Fig. 20) and designed the required tools and process parameter to obtain a tight mechanical interlock without fracture. The shear and peel tests were also simulated to reveal the mechanical properties and failure mechanisms of the novel hole-hemmed joint.

Considering the above circumstances, the prediction of fracture in the joining processes of dissimilar materials and the destructive tests of created joints can be point out as an interesting topic for future research. The development of fracture criteria appropriate to the deformation modes in the processes and the tests, as well as the development of calibration tests that can properly reflect these deformation modes, are among the items that need to be investigated.

3 Metallurgical joining by plastic deformation

The processes discussed so far are based on purely mechanical interlocks achieved by geometric changes. This change of geometry is obtained by plastic deformation performed at room temperature. FSW, which is classified as a solid-state welding process, is also based on plastic deformation. However, there are some key differences between the FSW and the aforementioned procedures that should be noted. First, the joining mechanism is based on metallurgical bonding, which is why it is classified as a welding process. Second, no geometric changes occur during the process, and third, plastic deformation occurs at a temperature above the recrystallization temperature. These cause some major differences with the processes based on mechanical locking in terms of evaluation methods of the joints. However, since the FSW process and the other plastic deformation-based joining processes are interchangeable for joining difficult-to-weld materials, they are discussed in a paper to provide readers with some useful criteria for process selection.

3.1 Process development

The development of a joining process is usually driven by the need to overcome its known limitations. In FSW, one of the most popular processes for metallurgical joining by plastic deformation, many of the issues are related to fixing of the workpieces. Among these issues are weld thinning, back support and key-hole formation [89]. Weld thinning is caused by the plunging of the tool into the workpieces. This plunging is necessary to provide the axial

load for sufficient material flow. The back support is needed to bear the axial load during welding. Key-hole formation is inevitable, as the tool retracts in the end and leaves behind a hole which is as large as the pin diameter. Other than these, kissing bond is also a common problem during FSW. This defect is characterized by a continuous oxide layer at the interface which is commonly formed at the root of the nugget zone [90]. Asymmetry in the weld zone, though is not considered as a defect, causes an inhomogeneity in the mechanical properties of the joint. This defect is due to different strain at advancing and retreating sides. Recently a Reverse Dual Rotation FSW (RDRFSW) was developed to overcome this problem by which the rotation directions of the pin and shoulder are opposite [91]. This process also helps to reduce the clamping requirements, as the torque imposed on the workpieces during FSW reduces by the counterpart rotation. The value of torque in FSW process is dependent on the material, thickness, tool geometry, tool dimensions, and the FSW parameters [92]. It will be shown that tracking the torque can give useful information about the quality of the process [93] and hence this parameter along with the other ones are used for online controlling of the process.

3.1.1 FSW tools

The FSW tool is the core element of the process that is composed of two main components, shoulder and pin. The first generation FSW tools were made of a concave shoulder which necessitates an inclination angle for trapping the plasticized material under the shoulder (Fig. 21 a). This would lead to some problems such as thinning of the workpiece. Furthermore, the complex paths and 3D dimensional curved paths cannot be joined by these tools. The second and third generations of the tools have been developed to overcome these problems [10]. The inward Archimedean profile on the shoulder of these tools helps to push the material inward (Fig. 21 b, c). In the second generation of the tools the shoulder is flat which is sensitive to the plunge depth and needs high assembly accuracy. In the third generation, the shoulder is convex which is less sensitive to the plunge depth and is more adaptable to the curved paths.

3.1.2 Friction stir spot welding (FSSW)

In this process, only the plunging, dwelling and retracting stages exist, meaning that the traversing of the tool is absent. This process is frequently used in joining dissimilar materials such as aluminium to copper [94], as the usual problems raised from intermetallic compound formation in FSW do not exist in FSSW. The existence of a hole is the main disadvantage of this process and therefore several procedures have been developed to overcome this problem. Refill friction stir welding uses a special designed tool to fill the hole whose schematic is presented in Fig. 22. The effectiveness of this process has been demonstrated for joining of dissimilar materials such as aluminium to steel [95]. In the case of dissimilar joining, a slight penetration into the bottom layer (which is chosen to be the harder material) is needed, in direct contrast to the similar welding in which the penetration into the bottom layer is high.

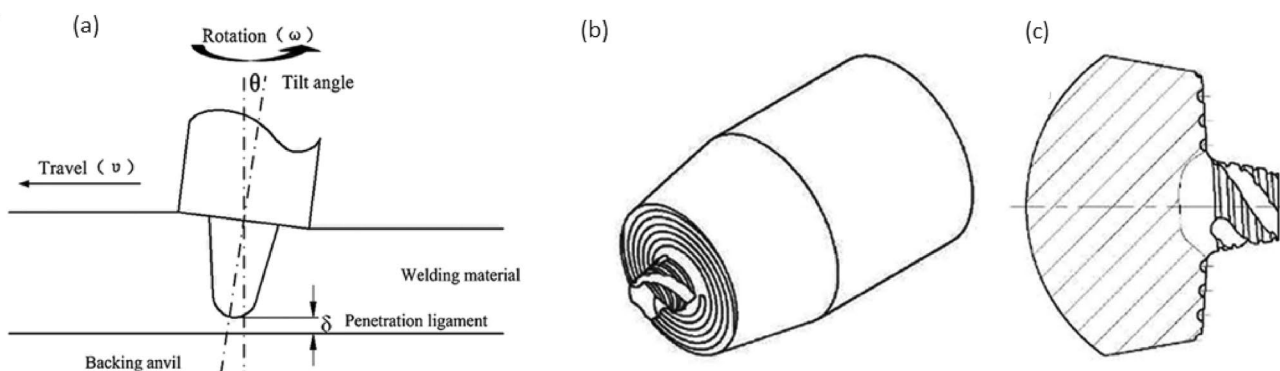
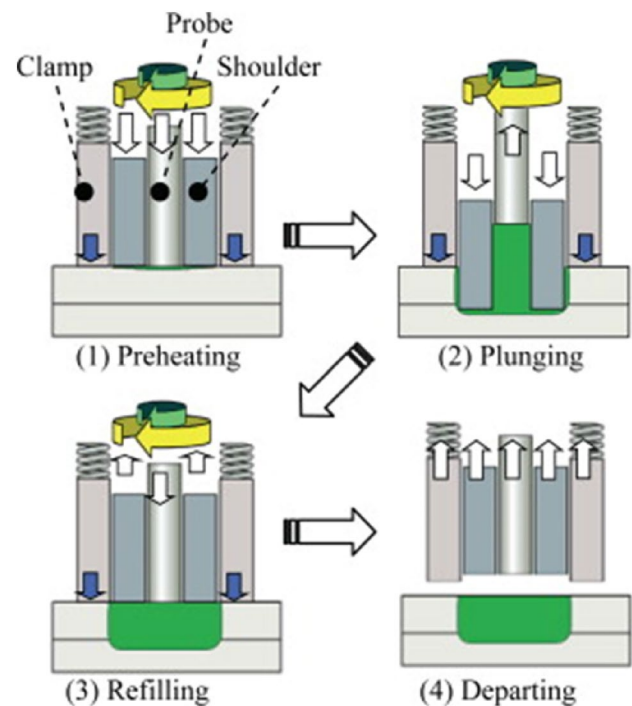


Fig. 21 a The inclination angle needed for first generation tools with concave shoulder. b, c the isometric side view and sectional view of third generation tools with convex shoulder and Archimedean spiral profile, respectively [10]. (Reprinted with permission from Elsevier)

Fig. 22 Refill friction stir welding [96]. (Reprinted with permission from Elsevier)



3.1.3 Self-reacting FSW (SRFSQ)

This process is a self-supportive FSW process which utilizes a bobbin tool consisting of two shoulders and a pin (see Fig. 23). In this process, also named as Bobbin-Tool FSW (BT-FSW), the need for axial load decreases, as there is another shoulder in the other side of the main shoulder which supports the work piece [89]. The thermal cycle in this process has more importance than that of conventional FSW due to more significant heat generation caused by the use of two shoulders. The vertical gap between the two shoulders, namely the Shoulder Pinching Gap, should be lower than the thickness of the material to provide a plunge depth of the upper and lower shoulder into the workpiece. This plunge depth, like conventional FSW, causes sufficient material flow and heat generation, whose absence causes the defect formation.

3.1.4 Penetrating FSW

This process utilizes a stationary shoulder with a blind hole to support the sheets from the back (Fig. 24). The end of the pin penetrates into this hole and the entire thickness of the sheets are touched by the pin, avoiding kissing bond formation at the root of the weld [97].

Fig. 23 The tool of **a** conventional and **b** BT-FSW

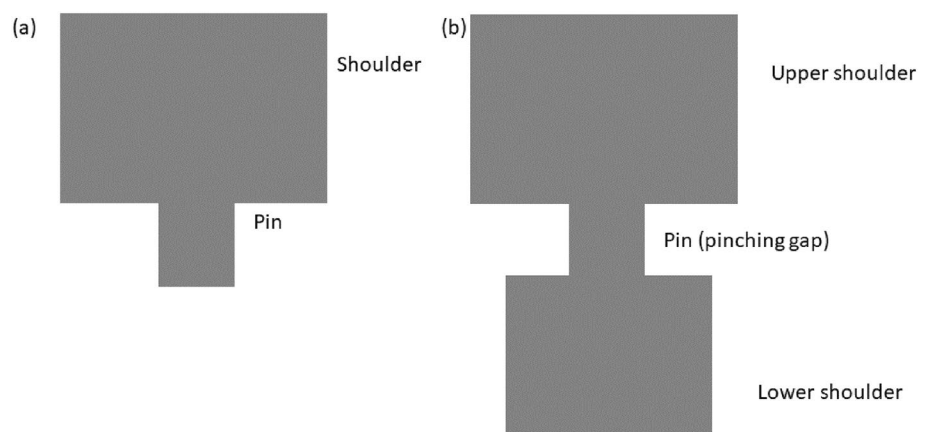
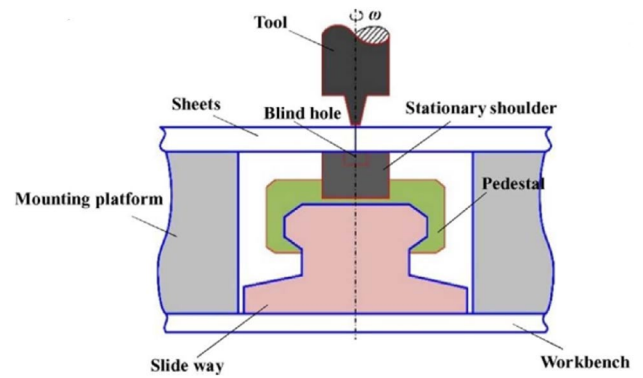


Fig. 24 Schematic of penetrating FSW process [97]. (Reprinted with permission from Elsevier)



3.1.5 Stationary shoulder friction stir welding (SSFSW)

This process uses a stationary shoulder which touches the upper surface but does not penetrate into the workpiece and therefore no thinning of the weld can occur [98]. Moreover, the heat generated by this method is controlled due to the absence of the rotation of the shoulder which suits it for cases where the heat conductivity is low like Ti [99] or for joining of dissimilar materials where the heat generation deteriorates the weld due to the formation of IMCs [100]. The reduction of IMC thickness and joint strength improvement [101] was observed during SSFSW of aluminium to copper [102]. It is also reported that a lower heat generation leads to a reduction in the residual stress during FSW of aluminium alloy [103]. SSFSW of Al6061 caused a uniform structure in the stir zone with a change in the texture with respect to the conventional FSW, which was attributed to the heat control [104].

3.1.6 Hot FSW

Hot FSW refers to those in which the temperature of the workpiece is intentionally raised during welding by additional processes. Hot FSW is used in the literature for various reasons. Joints made by FSW show a steep gradient of microstructure and hardness change in the advancing side, which is due to a high gradient of plastic strain. Li et al. [105] used TIG torch to preheat the front of the tool in the advancing side of an AA2219 alloy. This technique causes a smooth change in the microstructure and hardness along the weld line from the retreating side to the advancing side which consequently increases the joint strength. In cases where the melting point is high, such as steel, titanium, and nickel based super alloys, the heat generation during FSW is not high enough to cause plasticization and softening. Therefore, insufficient material flow may cause defect formation during welding [106]. To overcome this problem, a high rotation speed and a high axial load is needed which leads to severe wear of the tool [107]. External assisted FSW is used to provide additional heat to facilitate the softening of the material in order to reduce the required axial load and therefore reduce the wear of the tool [106]. Various methods of external heating are provided in the literature [106] such as induction assisted FSW, laser assisted FSW, electrically assisted FSW, arc assisted FSW and ultrasonic FSW. Raturi et al. [108] used a gas torch in front of the FSW tool to heat the aluminium alloys in order to change the texture and hardness of the weld nugget. A self-heated FSW tool was designed and fabricated to join polypropylene [109]. This heating caused better plasticization of the polymer and elimination of welding defects caused by insufficient material flow. A higher tensile strength of the joints was reported by using this technique.

3.1.7 Cold FSW

There are some purposes of cooling during FSW. Mahmoudiniya et al. [110] used a copper backing plate during FSW of DP700 (dual phase steel) to alleviate the softening in the HAZ. By doing so, both the tensile strength and elongation increased and the fracture location moved away from the HAZ to the base material. Aghajani et al. [111] used underwater FSW to join polycarbonate. The increased cooling rate caused the viscosity to be higher during FSW and a higher chemical stability and a lower crystallinity of the stir zone was obtained which led to an increase of the joint strength. FSW under cold condition is reported to help to stabilize the grain size in the stir zone of AA2519 aluminium alloy by keeping the peak temperature below the dissolution temperature of precipitates [112]. Preservation of precipitates caused the Zener pressure to be high enough during the subsequent annealing to prevent the abnormal grain growth. Other than

the precipitates, the initial grain size can also affect the stability of the grains. When the welding was performed in a cold condition by using a copper backing plate, the grains in the bottom were finer which provided the stored energy for abnormal grain growth during the subsequent heat treatment [113]. Therefore, a balance needs to be realized between the preservation of precipitates and grain refinement, as the former inhibits and the latter provokes the abnormal grain growth. Under-water FSW leads to a dark surface finish of aluminium alloys because of the oxidation reaction between hot aluminium and water [114]. Under-water FSW, due to its capability to lower the peak temperature, can prevent softening in AA6082 leading to a raise in the joint strength up to 10.7% with respect to the conventional FSW [115]. High speed FSW at 4 m/min was performed to join AA6063 aluminium alloy by which a fine grain structure was obtained in the stir zone [116]. However, due to high loads on the pin which cause the breakage a very high rotation speed is needed as well.

3.1.8 Mechanical locking

This mechanism is used when a metallurgical bond cannot be obtained, such as when welding a polymer to a metal. Although, not the main topic of this review, this mechanism is of note since it is also the dominant mechanism during similar welding of polymers [117]. Friction based filling stacking joining (FFSJ) was used by Huang et al. [118] to join a metal to polymer by filling a pre-fabricated hole in the metal with a stud. Friction stir dovetailing was used to join aluminium to steel by pre-fabricating a dovetail in steel and flowing of aluminium into it by FSW (Fig. 25). A part of this joint is metallurgical where an insert is in contact with steel, but the dominant mechanism of joining is mechanical interlocking.

3.2 Process monitoring

One of the most important characteristics of FSW machines is the high load bearing capacity of the spindle in the vertical direction. This vertical load is necessary to induce the flow of material in the workpieces during welding. To induce this axial load, an inclination angle of the tool with respect to the vertical axis is essential when concave tools are used [120]. Hence, special machines dedicated to FSW are needed to perform this process. CNC machines which are used for machining can also be adopted for FSW but with special consideration to the axial load. Imani et al. [121] developed a right angle FSW process by utilizing a flat shoulder with spirals to be used on a CNC machine. It was reported that the axial load is reduced which makes this process suited for CNC machine.

Online monitoring of FSW is used for some purposes such as predicting and controlling the weld defects [122] or adjusting the parameters during the process [123]. Various sensors can be implemented in the FSW machine to measure force, torque, current, power, temperature, vibration, acoustic emission, and imaging to use them for online controlling [124]. Appropriate features of these data should be extracted by Digital signal processing (DSP) and digital image processing (DIP) methods to be able to be used for online monitoring. Sudhager et al. [122] used the surface appearance of the welds made at various parameters to extract its features to be classified by support vector machine (SVM) with regard to the tensile strength. Stable Extremal Region (MSER) algorithm was used to extract the features of the welds successfully. Figure 26 shows the result of feature extraction of the weld surface to be used in SVM.

Fig. 25 Friction stir dovetailing of aluminium to steel [119]. (Reprinted with permission from Elsevier)

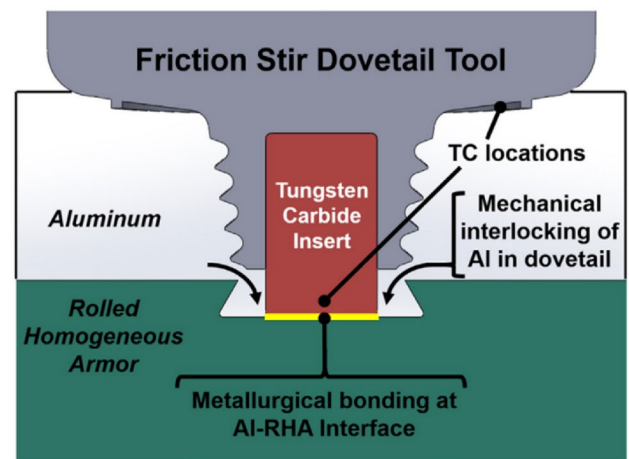
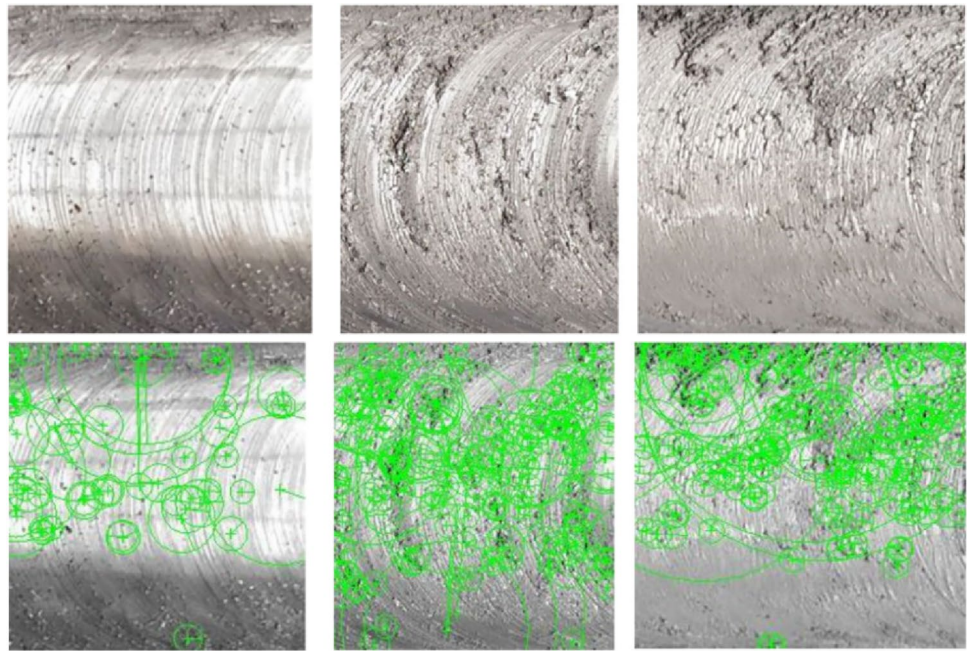


Fig. 26 Feature extraction of the weld surface to be used in SVM for online image processing of FSW [122]. (Reprinted with permission from Elsevier)



In addition to the surface appearance, the data obtained from various sensors can also be used for online monitoring of the process. These sensors provide information about the process in real time helping to control the process. Roy et al. [125] used the power signals of the spindle and found it effective in controlling the defects during FSW of aluminium alloys. A multi-sensor approach was used by Mishra et al. [126] where a graphical user interface (GUI) was created in Labview software to receive data from three sensors which measure force, torque and power. This data was transmitted from the sensors to a cloud and the weld parameters were transmitted from the cloud to the machine by TCP/IP interface. Discrete Wavelet Transform (DWT) was used by them to extract information from the obtained signals. These data were used in a trained artificial neural network (ANN) to predict the UTS. When the predicted UTS was higher than the expected value, the FSW was maintained with the same parameters otherwise new welding parameters are to be chosen from another trained ANN which are sent to the machine. Figure 27 shows the procedure of this online monitoring.

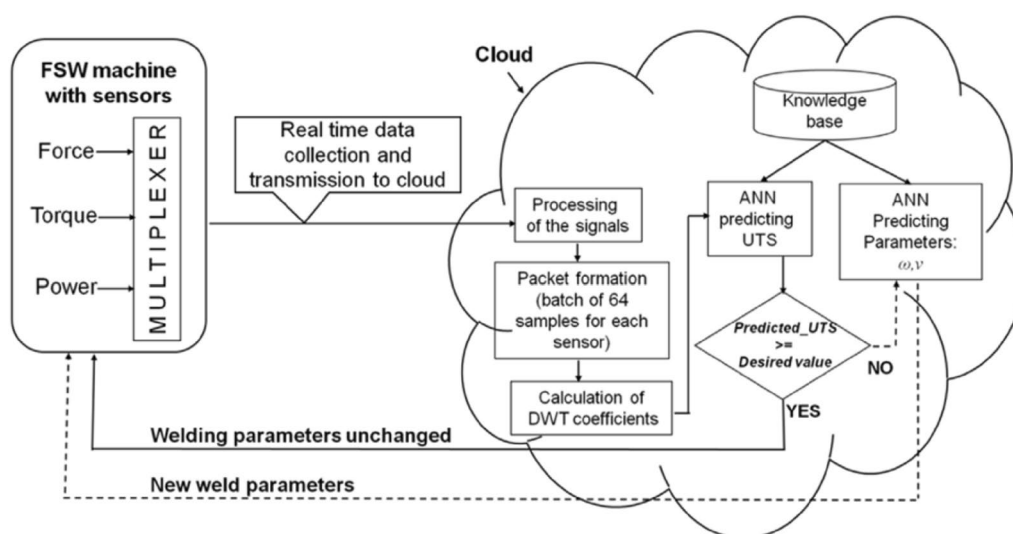


Fig. 27 The procedure of online monitoring of FSW by using the signals from various sensors [126]. (Reprinted with permission from Elsevier)

3.3 Process modelling

Modelling of the process helps to understand the effect of FSW parameters on thermal history and residual stress during FSW without the need to run several experiments [103]. Analytical solutions for calculating the temperature during FSW have been developed, so the need for the numerical simulation runs is avoided to a large extent. However, these formulations lack the potential to predict the material flow in FSW. Thermo-mechanical analysis of FSW is categorised in two approaches: Computational solid mechanics (CSM) and computational fluid mechanics (CFM) [127]. Flint et al. [128] proposed a volumetric heat source model to predict the spatial and temporal temperature during FSW. Their model, though fast and very efficient in modelling various stages of the process, is not as accurate as computational fluid dynamics (CFD) models. Bora et al. [129] developed an empirical formula to correlate the FSW variables with the peak temperature. They used a full-factorial design to do the FSW experiments and to obtain the peak temperature during each experiment. Finally, a mathematical model was developed which is helpful to predict the temperature at every FSW parameter. However, this mathematical model has several limitations. It can be used only for the selected material, tool, thickness and selected range of parameters. Furthermore, it cannot yield the spatial and temporal temperature in every point as it only yields the peak temperature only at a specific point. So, numerical solutions are still in a high demand to simulate the FSW process. Decoupled thermo-mechanical analysis is helpful for obtaining the residual stress and temperature distribution during the FSW, neglecting the material flow during the welding [130]. For material flow, a fully coupled model is needed by which the thermal process and the mechanical process are coupled.

The sole thermal modelling was also used by Sarikavak et al. [131] to understand the effect of FSW parameters on heat distribution during FSW of several materials. In their model they used the formulations which took rotation speed, weld speed and axial pressure into account to calculate the heat generation. In their model they did not consider directly the heat generated by plastic deformation. The heat generation by plastic deformation (q_p) is calculated according to the following equation [132]:

$$q_p = \beta \sigma \dot{\epsilon} \quad (1)$$

where β is a coefficient which describes the fraction of the plastic deformation work converted to heat, σ is the equivalent stress and $\dot{\epsilon}$ is the strain rate.

Three approaches Lagrangian, Eulerian and arbitrary Lagrangian–Eulerian (ALE) formulations can be chosen for finite element simulation [109]. In Lagrangian formulation the meshes are attached to the material and the meshes follow the material deformation which seems appropriate for FSW in which severe plastic deformation exists. However, large strains cause large distortion and to avoid this, very small step sizes are needed. In Eulerian formulation, the meshes are fixed and the material flows through the faces of the elements which is beneficial in avoiding the complications during simulation of large strains. This formulation needs a prior knowledge of the tool/workpiece contact length and geometry and it cannot resolve the flow detail which limits its application. It is mainly used in fluid dynamics [133]. ALE is developed to overcome the shortcomings of two approaches and can be used in large deformation problems. However, this method encounters divergence of numerical solution when excessive mesh distortion exists [134]. Coupled Eulerian–Lagrangian (CEL) method is reliably used to simulate the FSW process by which the tool is formulated as Lagrangian and the workpiece is formulated as Eulerian [135]. In this method, the interaction between the tool-workpiece is very important as it determines the material flow and heat generation [136]. Generally, the tool-workpiece interaction is a combination of sticking and slipping whose participations depend on several factors [137]. The Lagrangian body should be coupled with the Eulerian tool with a contact interaction (for example the Coulomb friction law). The higher the friction coefficient of the tool/workpiece the higher is the sticking dominant zone, as verified by an analytical model developed by Wang et al. [138].

In CFD approach the material is considered as non-Newtonian fluid and the conservation equation of mass, momentum, and energy for viscous fluid are used for analysing the thermo mechanical behaviour in FSW [127]. CFD needs less computational time with respect to CEL but the thermo mechanical fields obtained by CEL are more reliable [138]. Aghajani et al. [111] used CFD to model the material flow during FSW of polycarbonate both in the air and under the water. The viscosity of the polymer was related to the temperature and strain rate whose alteration during FSW and under-water FSW determined the material flow and the defect formation. Zhao et al. [139] used a pressure-dependent velocity boundary condition by which the effect of the welding speed on the shape of the stir zone could be accurately captured.

Smoothed particle hydrodynamic is another approach used to simulate the material flow during welding to predict the defect formation [140]. This method is mesh-less and the computational units are nodes instead of elements, eliminating the risk of element distortion [141].

3.4 Joint evaluation

3.4.1 Mechanical behaviour

The determinant factors in joint strength are of different nature in similar and dissimilar welding. In dissimilar welding, the mixing pattern of two materials as well as the formation of intermetallic compounds play the major role in mechanical properties [142]. In similar welding the softening due to recrystallization and the kissing bond are the critical factors [143]. In the welds made by bobbin tool FSW a S-line defect appeared in the nugget zone which acted as the fracture site which is attributed to insufficient fragmentation of oxide layer at the faying surface [132]. In the spot welds made by FSSW the failure occurs in the joint area due to the stress and strain concentration around the hole which is inherent to the process [144]. In dissimilar welds the thickness and distribution of intermetallic compounds determine the joint strength, making the fracture behaviour to be brittle in most cases [145].

3.4.2 Metallographic examination

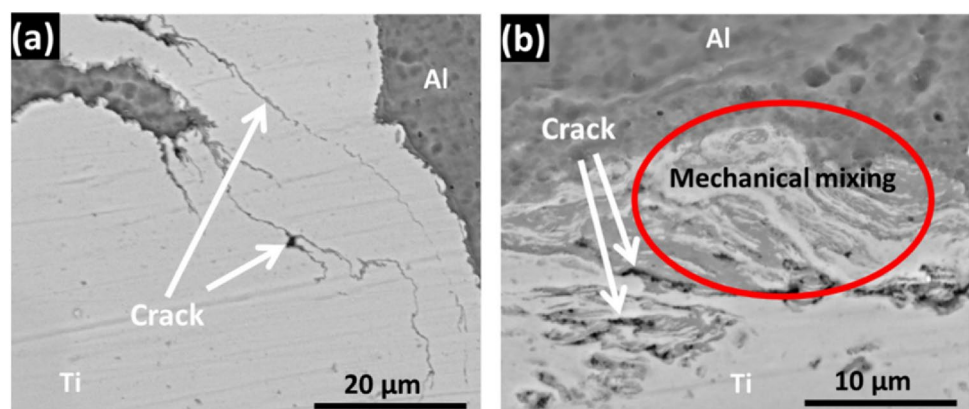
Metallography is usually used in both macro and micro scales. The macro scale images are used to observe the shape and the extent of the nugget and HAZ as well as the macro defects. The macro defect such as voids are usually formed in the junction of different flow zones [146]. It seems that when the frontier of the flow zones is not well consolidated in the junction, defects appear. The macrostructure image of the nugget formed by BT-FSW is symmetric in the upper and lower part due to the usage of two shoulders in both sides [147]. The macrostructure of a weld obtained by SSFSW misses the shoulder affected zone region and the widths of HAZ and TMAZ are reduced due to the reduced heat input [148].

3.4.3 Electron microscopy

Transmission electron microscopy (TEM) is usually used to observe the precipitates, subgrain boundaries, and dislocations. This method is especially useful for precipitation hardening aluminium alloys in which the precipitates of different regions undergo different evolutions. In TMAZ of aluminium, the precipitates can be coarsened [149] or remain which depends on the peak temperature during the welding.

Scanning Electron Microscopy (SEM) is used to observe the distribution and morphology of phases especially in the case of dissimilar welding. In this case, Back Scattered Electron (BSE) mode is helpful, as it provides a contrast of chemical composition in a grey scale. Dissimilar joining by FSW is mostly concerned with joining of Al with other materials such as copper, steel, magnesium, and titanium. The fragments of a material inside the other caused by the FSW tool rotation can be discernible by this method giving a good understanding of the process mechanism [150]. Figure 28a, b show the distribution of two Al and Ti at the interface and the stir zone of a join between these two metals. The micro cracks are also observable in the stir zone which are associated with intermetallic compounds formation. The formation

Fig. 28 BSE image of the interface of Al and Ti joined by FSW showing: **a** the weld interface and **b** the mixing region and cracks in the stir zone [152]. (Reprinted with permission from Elsevier)



of intermetallic compounds occurs in the case of dissimilar materials and their distribution and morphology and size are very important in determination of the mechanical properties of the joints. The Secondary Electron is useful in the study of fracture surface whose topology gives useful information about the mechanism of fracture [151].

3.4.4 Electron back scatter diffraction (EBSD) observations

EBSD is a strong tool to observe the texture, misorientation, and grain size. EBSD is a powerful tool to study the mechanism of joining in FSW, as plastic deformation is the main mechanism in the process. This process is associated with recrystallization phenomenon whose mechanism can be estimated by EBSD results. In the case of aluminium alloys, every recrystallization mechanism is associated with a specific texture. For example, cube texture is a characteristic of discontinuous dynamic recrystallization [153]. Development of texture during FSW is attributed to the self-adaption of the crystallographic orientations by which the lowest energy for plastic flow is needed [154]. Imam et al. [155] used EBSD technique to study the texture around the FSW tool. They attributed the high angle grain boundaries to the mechanism of particle stimulated nucleation by which a random texture develops. Raturi et al. [108] used EBSD technique to study the effect of assisted heating on the misorientation distribution and texture in the advancing and the retreating sides of the friction stir welded aluminium alloys. They observed an increase in the high angle grain boundary fraction when using the heating (see Fig. 29).

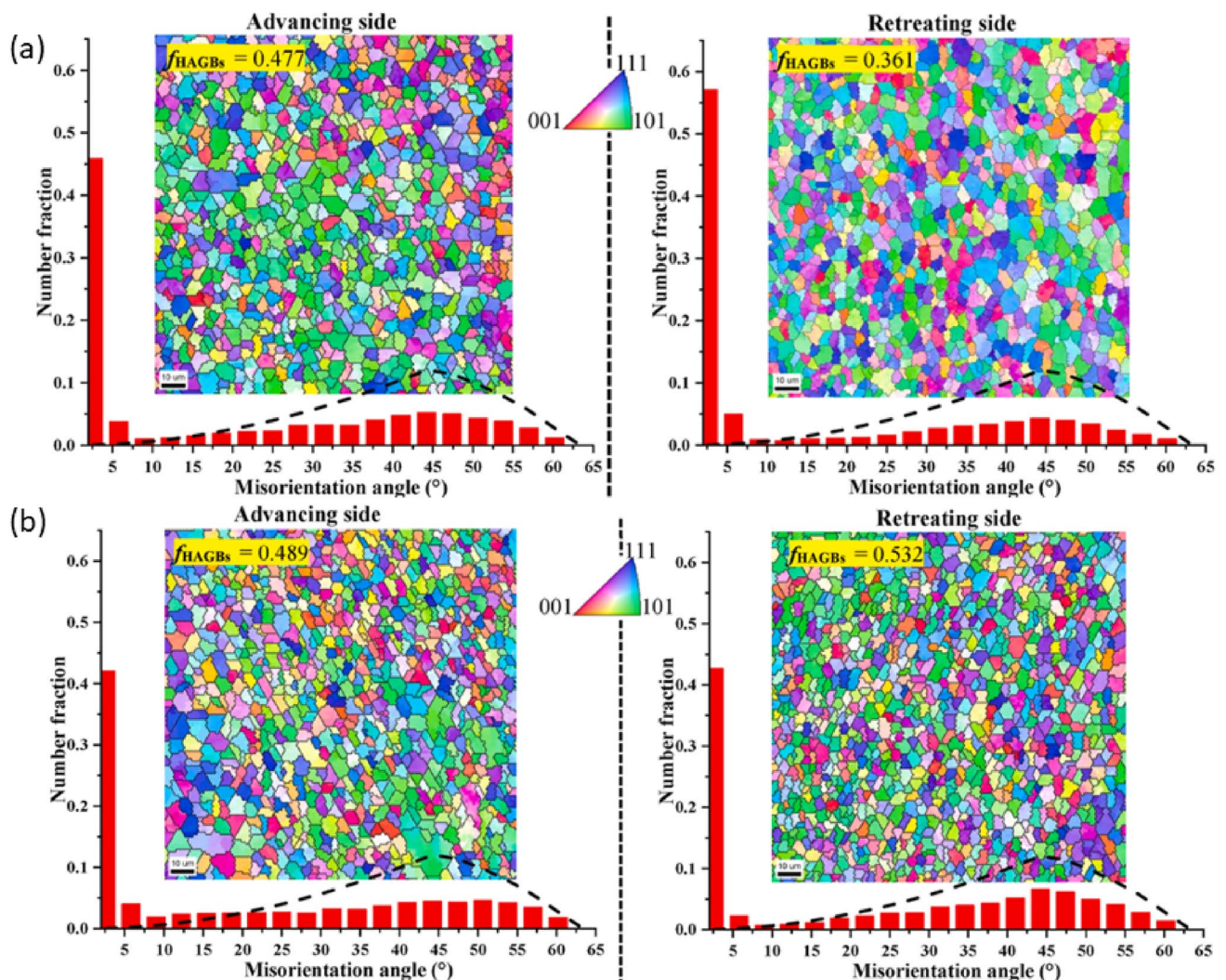


Fig. 29 IPF and GB distribution of FSWed aluminum alloys: **a** without heating and **b** with heating [108]. (Reprinted with permission from Elsevier)

The texture developed during FSW is critical in determination of the joint properties in Mg alloys which possess a hexagonal close-packed (HCP) structure. A strong 0001 texture is developed in the stir zone of Mg alloys whose tilting with respect to the applied load during the mechanical testing is determinant. When this texture is inclined 48° with respect to the applied load, the yield stress decreases, because the shear load in these planed would be maximum [156]. Zhang et al. [157] showed that by post processing of the weld nugget by TIG welding the ductility of the joints increases which was attributed to the change of texture to a more random one. This is because in HCP structures, due to limitation of the active slipping systems for plastic deformation, the presence of texture limits the plasticity and therefore the ductility.

4 A general comparison of the processes

In order to have criteria for the selection of joining processes by plastic deformation, the advantages and disadvantages of these processes must be compared. In this regard, several aspects are taken into account as can be seen in Table 1. Most sheet materials including metals, polymers and composites can be joined at least by one of the mechanical joining processes by plastic deformation and there is no limit to coated and painted sheets.

In these processes, samples do not require preparation except for those that make an interlock through a pre-hole like the hole clinching process. In FSW process, no special preparation is needed for both butt and lap configurations. After designing a mechanical-based joining process by engineers, low-skilled operators can carry out joining operations. In FSW process, the technician must be trained well for both fixturing, tool selection, and setting the FSW parameters. The geometry of the tool, the tool rotation speed, the tool offset in the material (especially in the case of dissimilar ones) need to be chosen properly in order to obtain a sound joint. The forming force required in the mechanical-based joining methods is high due to cold plastic deformation applied to a small region. As a result of this, materials with high strength need to be selected for required tools, especially when one of the joining components is made of high strength materials. Compared to FSW process, the mechanical-based joining methods requires more complex tools. For FSW process, the tools can be made of cheap tool-steels when the light material such as aluminium and magnesium are involved in the joining process. In special cases such as joining of steels or titanium, the tools need to be made of expensive materials such as carbide-tungsten or Polycrystalline cubic boron nitride (PCBN). The initial investment for the equipment for mechanical-based joining methods is low and they can be usually performed on regular machines in industries. It is also possible to design portable equipment and tools for them to be used simply and quickly in production lines. The price of the FSW machine is relatively high which is dependent on the volume of the work, material, and thickness. One main advantage of the FSW process is that it can perform continuous, seamless joints while this is not possible in the case of mechanical-based joining methods. The FSW process is very sensitive to the parameters and several defects may appear during welding. As mentioned, the technician needs to be well trained to select the optimum parameters for each case. The mechanical joining processes are less sensitive to their parameters because deformation occurs at ambient temperature and there is no need to create a metallurgical connection.

Table 1 Comparative characteristics of the joining methods by plastic deformation

Processes	Mechanical-based methods	Metallurgical-based method (FSW)
Materials	Most sheet materials (metals, polymers and composites)	All deformable materials
Sample preparation	Low	Low
Skill level required	Low	High
Tool cost	High	Low for light alloys
Fixtures needed	Low	High
Equipment cost	Low	High
Continuous seamless joint	No	Yes
Portability	High	Low
Sensitivity to process parameters	Low	High

5 Summary and future perspective

In the present study, two joining technologies based on plastic deformation that can be used for manufacturing multi-material structures are discussed. Joining by plastic deformation, such as clinching, self-pierce riveting and other innovative processes, creates a mechanical bond between two materials and is capable of joining any pair of materials including metals, polymers and composites, at least one of which is deformable. The preparation techniques for these processes are not complex and costly. These processes are fast and do not need post processing. The change in microstructure during these processes is negligible and confined to a limited area. These processes are considered a spot joint and therefore cannot join a seam. Furthermore, a lap configuration is needed for them to make a joint. The FSW process, on the other hand, is based on a metallurgical bond produced by severe plastic deformation. With the FSW, the mechanical interlock, if present, has no significant contribution in the joining process, unless the process is designed to do so. FSW processes need robust fixturing due to the high torque of the tool in the materials. The microstructural changes in materials joined by FSW are high and can affect the quality of the joint. Hence, the characterization techniques such as optical and electron microscopy are frequently used to evaluate these joints. These techniques are not used to evaluate joints made by mechanical interlocking because the microstructural changes are less important than the geometric ones.

The review of previous researches revealed that mechanical joining by plastic deformation, especially in recent years, is being extensively developed, which is actually a response to the growing needs for the sustainable manufacturing of the lightweight structures from advanced materials in the transportation sector. However, several challenges remain to be addressed. The flexibility of the mechanical joining processes based on plastic deformation is one of the topics that needs to be investigated in order to be able to connect new material combinations with the lowest cost and time. Joining metals with very different mechanical properties faces serious challenges, such as joining metals that have low ductility (e.g., magnesium), or have very high strength, (e.g., advanced high-strength steels) to other metals. There is also a need for processes that can effectively connect metals to composites and polymers. With the growing development of printed materials, focus should be also placed on the connection of this type of materials. The hybrid processes showed that they are able to produce high-quality joints and, therefore, can be further developed to overcome some above-mentioned challenges. The evaluation of joints under loading conditions existing in industrial applications such as dynamic and cyclic loadings need to be given more attention in order to gain the confidence of industries for the use of these joints. Appropriate fracture models alongside their calibration tests should be developed for the joining processes of dissimilar materials and the destructive tests of joints in order to provide more accurate predictions for the process design and the joint evaluation. Due to the potential interchangeability of FSW and other processes mentioned, in addition to evaluating machining properties, life cycle analyses must be performed to provide comprehensive criteria for process selection that also consider environmental impacts and economic aspects.

Acknowledgements Mohammad Mehdi Kasaei gratefully acknowledges the funding provided by operation NORTE-06-3559-FSE-000107—Contratação de Recursos Humanos Altamente Qualificados (PME ou CoLAB), supported by Norte 2020 through Fundo Social Europeu.

Author contributions RB, MMK, EASM, RJCC contributed to the manuscript preparation. LFMDS made the supervision. All the authors reviewed the article. All authors read and approved the final manuscript.

Data availability Data sharing is not applicable to this article as no new data were created or analyzed in this study.

Declarations

Competing interests The authors declare no competing interests.

Open Access This article is licensed under a Creative Commons Attribution 4.0 International License, which permits use, sharing, adaptation, distribution and reproduction in any medium or format, as long as you give appropriate credit to the original author(s) and the source, provide a link to the Creative Commons licence, and indicate if changes were made. The images or other third party material in this article are included in the article's Creative Commons licence, unless indicated otherwise in a credit line to the material. If material is not included in the article's Creative Commons licence and your intended use is not permitted by statutory regulation or exceeds the permitted use, you will need to obtain permission directly from the copyright holder. To view a copy of this licence, visit <http://creativecommons.org/licenses/by/4.0/>.

References

1. Czerwinski F. Current trends in automotive lightweighting strategies and materials. *Materials*. 2021;14(21):6631.
2. Lipman TE, Maier P. Advanced materials supply considerations for electric vehicle applications. *MRS Bull.* 2021;46(12):1164–75. <https://doi.org/10.1557/s43577-022-00263-z>.
3. Gite RA, Loharkar PK, Shimpi R. Friction stir welding parameters and application: a review. *Mater Today Proc.* 2019;19:361–5. <https://doi.org/10.1016/j.matpr.2019.07.613>.
4. Magalhães VM, Leitão C, Rodrigues DM. Friction stir welding industrialisation and research status. *Sci Technol Weld Join.* 2018;23(5):400–9. <https://doi.org/10.1080/13621718.2017.1403110>.
5. Singh K, Singh G, Singh H. Investigation on the microstructure and mechanical properties of a dissimilar friction stir welded joint of magnesium alloys. *Proc Inst Mech Eng Part L J Mater Des Appl.* 2019;233(12):2444–54. <https://doi.org/10.1177/1464420719865292>.
6. Radisavljevic I, Zivkovic A, Radovic N, Grabulov V. Influence of FSW parameters on formation quality and mechanical properties of Al 2024-T351 butt welded joints. *Trans Nonferrous Met Soc China.* 2013;23(12):3525–39. [https://doi.org/10.1016/S1003-6326\(13\)62897-6](https://doi.org/10.1016/S1003-6326(13)62897-6).
7. Alimadadi M, Mahmoudiniya M, Goodarzi M, Boutorabi SMA. Effect of tool transverse speed and pin offset on the properties of friction stir welding Al6061-St52 dissimilar joint. *J Adv Join Process.* 2022;5:100116. <https://doi.org/10.1016/j.jajp.2022.100116>.
8. Huang Y, Huang T, Wan L, Meng X, Zhou L. Material flow and mechanical properties of aluminum-to-steel self-rieveting friction stir lap joints. *J Mater Process Technol.* 2019;263:129–37. <https://doi.org/10.1016/j.jmatprotec.2018.08.011>.
9. Evans WT, Gibson BT, Reynolds JT, Strauss AM, Cook GE. Friction stir extrusion: a new process for joining dissimilar materials. *Manuf Lett.* 2015;5:25–8. <https://doi.org/10.1016/j.mfglet.2015.07.001>.
10. Wang G, Zhao Y, Hao Y. Friction stir welding of high-strength aerospace aluminum alloy and application in rocket tank manufacturing. *J Mater Sci Technol.* 2018;34(1):73–91. <https://doi.org/10.1016/j.jmst.2017.11.041>.
11. Hussein SA, Tahir ASM, Hadzley AB. Characteristics of aluminum-to-steel joint made by friction stir welding: a review. *Mater Today Commun.* 2015;5:32–49.
12. Bielak CR, Böhnke M, Beck R, Bobbert M, Meschut G. Numerical analysis of the robustness of clinching process considering the pre-forming of the parts. *J Adv Join Process.* 2021;3:100038. <https://doi.org/10.1016/j.jajp.2020.100038>.
13. Lee C-J, Lee J-M, Ryu H-Y, Lee K-H, Kim B-M, Ko D-C. Design of hole-clinching process for joining of dissimilar materials—Al6061-T4 alloy with DP780 steel, hot-pressed 22MnB5 steel, and carbon fiber reinforced plastic. *J Mater Process Technol.* 2014;214(10):2169–78. <https://doi.org/10.1016/j.jmatprotec.2014.03.032>.
14. Liu Y, Zhuang W, Wu S. Damage to carbon fibre reinforced polymers (CFRP) in hole-clinched joints with aluminium alloy and CFRP. *Compos Struct.* 2020;234:111710. <https://doi.org/10.1016/j.compstruct.2019.111710>.
15. Lee C-J, Kim B-M, Kang B-S, Song W-J, Ko D-C. Improvement of joinability in a hole clinching process with aluminum alloy and carbon fiber reinforced plastic using a spring die. *Compos Struct.* 2017;173:58–69. <https://doi.org/10.1016/j.compstruct.2017.04.010>.
16. Meschut G, Merklein M, Brosius A, Drummer D, Fratini L, Füssel U, et al. Review on mechanical joining by plastic deformation. *J Adv Join Process.* 2022;5:100113. <https://doi.org/10.1016/j.jajp.2022.100113>.
17. Hörhold R, Müller M, Merklein M, Meschut G. Mechanical properties of an innovative shear-clinching technology for ultra-high-strength steel and aluminium in lightweight car body structures. *Weld World.* 2016;60(3):613–20. <https://doi.org/10.1007/s40194-016-0313-0>.
18. Wiesenmayer S, Merklein M. Investigation of the joinability of the high-strength aluminum alloy AA7075 in shear-clinching processes. *Proc Inst Mech Eng Part L J Mater Des Appl.* 2022;236(6):1236–45. <https://doi.org/10.1177/14644207211067935>.
19. Wiesenmayer S, Merklein M. Potential of shear-clinching technology for joining of three sheets. *J Adv Join Process.* 2021;3:100043. <https://doi.org/10.1016/j.jajp.2021.100043>.
20. Lambiase F. Joinability of different thermoplastic polymers with aluminium AA6082 sheets by mechanical clinching. *Int J Adv Manuf Technol.* 2015;80(9):1995–2006. <https://doi.org/10.1007/s00170-015-7192-1>.
21. Krassmann D, Moritzer E. Development of a new joining technology for hybrid joints of sheet metal and continuous fiber-reinforced thermoplastics. *Weld World.* 2022;66(1):45–60. <https://doi.org/10.1007/s40194-021-01194-0>.
22. Qin D, Chen C. Research on the mechanical property and failure mechanism of the dieless clinched joints of various aluminum alloys. *Eng Fail Anal.* 2022;137:106384. <https://doi.org/10.1016/j.engfailanal.2022.106384>.
23. Qin D, Chen C. Research on the joining of dissimilar aluminum alloys by a dieless clinching process. *Int J Adv Manuf Technol.* 2022;122(5):2529–42. <https://doi.org/10.1007/s00170-022-09960-0>.
24. Atia MKS, Jain MK. A novel approach to hot die-less clinching process for high strength AA7075-T6 sheets. *Proc Inst Mech Eng C J Mech Eng Sci.* 2020;234(19):3809–25. <https://doi.org/10.1177/0954406220917406>.
25. Neugebauer R, Kraus C, Dietrich S. Advances in mechanical joining of magnesium. *CIRP Ann.* 2008;57(1):283–6. <https://doi.org/10.1016/j.cirp.2008.03.025>.
26. Friedrich S, Gerstmann T, Binotsch C, Awiszus B. Numerical and experimental investigation of flat-clinch joint strength. *Prod Eng Res Devel.* 2022;16(2):275–84. <https://doi.org/10.1007/s11740-021-01101-y>.
27. Wu J, Chen C. Investigation on clinch riveting process with different material combinations. *Proc Inst Mech Eng Part L J Mater Des Appl.* 2022;236(12):2455–66. <https://doi.org/10.1177/14644207221094930>.
28. Chen C, Zhang X, Wen C, Yin Y. Effect of blank holder force on joining quality of the flat clinch-rivet process. *Int J Adv Manuf Technol.* 2022;121(9):6315–23. <https://doi.org/10.1007/s00170-022-09744-6>.
29. Peng H, Chen C, Ren X, Ran X, Gao X. Research on the material flow and joining performance of two-strokes flattening clinched joint. *Thin Walled Struct.* 2021;169:108289. <https://doi.org/10.1016/j.tws.2021.108289>.
30. Qin D, Chen C, Li H, Ren X. Investigation of the novel two-step flat clinching process to achieve double-sided flat surfaces on engineering structures. *J Braz Soc Mech Sci Eng.* 2022;44(11):525. <https://doi.org/10.1007/s40430-022-03809-z>.
31. Zhang P, Chen C, Zhang C-W, Cao Y-F, Li S-J, Li F, et al. Novel technique of friction extrusion self-refilling for repairing keyhole of flat clinched joint. *Int J Mech Sci.* 2022;233:107658. <https://doi.org/10.1016/j.ijsmecsci.2022.107658>.

32. Zheng C, Pan C, Wang J, Zhao G, Ji Z. Mechanical joining behavior of Cu–Fe dissimilar metallic foils in laser shock clinching. *Int J Adv Manuf Technol.* 2020;110(3):1001–14. <https://doi.org/10.1007/s00170-020-05920-8>.
33. Hou Y, Ding K, Lu G, Zheng C, Ji Z. Investigation of microscale laser shock flat hole clinching. *Int J Precis Eng Manuf.* 2022;23(9):1019–25. <https://doi.org/10.1007/s12541-022-00665-8>.
34. Yuan H, Pan C, Song L, Zhao G, Zheng C. Modeling and optimization of laser shock hole-clinching using response surface methodology and genetic algorithm. *Int J Adv Manuf Technol.* 2022;122(5):2391–406. <https://doi.org/10.1007/s00170-022-10056-y>.
35. Ma Y, Abe Y, Geng P, Akita R, Ma N, Mori K-I. Adhesive dynamic behavior in the clinch-bonding process of aluminum alloy A5052-H34 and advanced high-strength steel JSC780. *J Mater Process Technol.* 2022;305:117602. <https://doi.org/10.1016/j.jmatprotec.2022.117602>.
36. Abe Y, Maeda T, Yoshioka D, Mori K-I. Mechanical clinching and self-pierce riveting of thin three sheets of 5000 series aluminium alloy and 980 MPa grade cold rolled ultra-high strength steel. *Materials.* 2020;13(21):4741.
37. Gerstmann T, Awiszus B. Hybrid joining: numerical process development of flat-clinch-bonding. *J Mater Process Technol.* 2020;277:116421. <https://doi.org/10.1016/j.jmatprotec.2019.116421>.
38. Wang Y, Lu G, Ji Z, Liu R, Zheng C. The small-size laser shock adhesive-clinching of Al foils. *Int J Adv Manuf Technol.* 2022;122(9):3837–48. <https://doi.org/10.1007/s00170-022-10123-4>.
39. Li D, Chrysanthou A, Patel I, Williams G. Self-piercing riveting—a review. *Int J Adv Manuf Technol.* 2017;92(5):1777–824. <https://doi.org/10.1007/s00170-017-0156-x>.
40. Zhao H, Han L, Liu Y, Liu X. Analysis of joint formation mechanisms for self-piercing riveting (SPR) process with varying joining parameters. *J Manuf Process.* 2022;73:668–85. <https://doi.org/10.1016/j.jmapro.2021.11.038>.
41. Kappe F, Zirngibl C, Schleich B, Bobbert M, Wartzack S, Meschut G. Determining the influence of different process parameters on the versatile self-piercing riveting process using numerical methods. *J Manuf Process.* 2022;84:1438–48. <https://doi.org/10.1016/j.jmapro.2022.11.019>.
42. Mori K-I, Abe Y. A review on mechanical joining of aluminium and high strength steel sheets by plastic deformation. *Int J Lightw Mater Manuf.* 2018;1(1):1–11. <https://doi.org/10.1016/j.ijlmm.2018.02.002>.
43. Abe Y, Kato T, Mori K. Self-piercing riveting of high tensile strength steel and aluminium alloy sheets using conventional rivet and die. *J Mater Process Technol.* 2009;209(8):3914–22. <https://doi.org/10.1016/j.jmatprotec.2008.09.007>.
44. Mori K, Kato T, Abe Y, Ravshanbek Y. Plastic joining of ultra high strength steel and aluminium alloy sheets by self piercing rivet. *CIRP Ann.* 2006;55(1):283–6. [https://doi.org/10.1016/S0007-8506\(07\)60417-X](https://doi.org/10.1016/S0007-8506(07)60417-X).
45. Kuball C-M, Uhe B, Meschut G, Merklein M. Process-adapted temperature application within a two-stage rivet forming process for high nitrogen steel. *Proc Inst Mech Eng Part L J Mater Des Appl.* 2022;236(6):1285–301. <https://doi.org/10.1177/14644207211068693>.
46. Ma Y, Yang B, Lou M, Li Y, Ma N. Effect of mechanical and solid-state joining characteristics on tensile-shear performance of friction self-piercing riveted aluminum alloy AA7075-T6 joints. *J Mater Process Technol.* 2020;278:116543. <https://doi.org/10.1016/j.jmatprotec.2019.116543>.
47. Ma YW, Li YB, Lin ZQ. Joint formation and mechanical performance of friction self-piercing riveted aluminum alloy AA7075-T6 joints. *J Manuf Sci Eng.* 2019;141(4). <https://doi.org/10.1115/1.4042568>.
48. Shan H, Ma Y, Niu S, Yang B, Lou M, Li Y, et al. Friction stir riveting (FSR) of AA6061-T6 aluminum alloy and DP600 steel. *J Mater Process Technol.* 2021;295:117156. <https://doi.org/10.1016/j.jmatprotec.2021.117156>.
49. Ferreira FR, Pragança JPM, Bragança IMF, Silva CMA, Martins PAF. Injection lap riveting. *CIRP Ann.* 2021;70(1):261–4. <https://doi.org/10.1016/j.cirp.2021.03.018>.
50. Wituschek S, Lechner M. Investigation of the influence of the tumbling angle on a tumbling self-piercing riveting process. *Proc Inst Mech Eng Part L J Mater Des Appl.* 2022;236(6):1302–9. <https://doi.org/10.1177/14644207221080068>.
51. Wituschek S, Kappe F, Lechner M. Investigation of the influence of varying tumbling strategies on a tumbling self-piercing riveting process. *Prod Eng Res Devel.* 2022;16(2):353–62. <https://doi.org/10.1007/s11740-021-01099-3>.
52. Wituschek S, Kappe F, Meschut G, Lechner M. Geometric and mechanical joint characterization of conventionally and tumbled self-piercing riveting joints. *Proc Inst Mech Eng Part L J Mater Des Appl.* 2022. <https://doi.org/10.1177/14644207221135400>.
53. Kato K, Okamoto M, Yasuhara T. Method of joining sheets by using new type rivets. *J Mater Process Technol.* 2001;111(1):198–203. [https://doi.org/10.1016/S0924-0136\(01\)00519-2](https://doi.org/10.1016/S0924-0136(01)00519-2).
54. Alves LM, Afonso RM, Pereira PT, Martins PAF. Double-sided self-pierce riveting of dissimilar materials. *Int J Adv Manuf Technol.* 2021;115(11):3679–87. <https://doi.org/10.1007/s00170-021-07426-3>.
55. Alves LM, Afonso RM, Pereira PT, Martins PAF. Double-sided self-pierce riveting with flat-bottom holes: a feasibility study. *Prod Eng Res Devel.* 2022;16(2):401–9. <https://doi.org/10.1007/s11740-021-01082-y>.
56. Lambiase F, Scipioni SI, Lee C-J, Ko D-C, Liu F. A state-of-the-art review on advanced joining processes for metal-composite and metal-polymer hybrid structures. *Materials.* 2021;14(8):1890.
57. Liu Y, Zhuang W, Luo Y, Xie D, Mu W. Joining mechanism and damage of self-piercing riveted joints in carbon fibre reinforced polymer composites and aluminium alloy. *Thin-Walled Struct.* 2023;182:110233. <https://doi.org/10.1016/j.tws.2022.110233>.
58. Wang J, Zhang G, Zheng X, Li J, Li X, Zhu W, et al. A self-piercing riveting method for joining of continuous carbon fiber reinforced composite and aluminum alloy sheets. *Compos Struct.* 2021;259:113219. <https://doi.org/10.1016/j.compstruct.2020.113219>.
59. Zhang X, He X, Xing B, Wei W, Lu J. Pre-holed self-piercing riveting of carbon fibre reinforced polymer laminates and commercially pure titanium sheets. *J Mater Process Technol.* 2020;279:116550. <https://doi.org/10.1016/j.jmatprotec.2019.116550>.
60. Rao Z, Ou L, Wang Y, Wang P-C. A self-piercing-through riveting method for joining of discontinuous carbon fiber reinforced nylon 6 composite. *Compos Struct.* 2020;237:111841. <https://doi.org/10.1016/j.compstruct.2019.111841>.
61. Vorderbrüggen J, Meschut G. Investigations on a material-specific joining technology for CFRP hybrid joints along the automotive process chain. *Compos Struct.* 2019;230:111533. <https://doi.org/10.1016/j.compstruct.2019.111533>.
62. Liu Y, Han L, Zhao H, Liu X. Numerical modelling and experimental investigation of the Riv-Bonding process. *J Mater Process Technol.* 2021;288:116914. <https://doi.org/10.1016/j.jmatprotec.2020.116914>.
63. Charalampidou C-M, Braga DFO, Bergmann L, Kourkoulis SK, da Silva LFM, Infante V, et al. The effect of prior adhesive bonding on the corrosion behavior of AA2024 FSWed single lap joints. *Mech Mater.* 2022;164:104122. <https://doi.org/10.1016/j.mechmat.2021.104122>.

64. Huang Z-C, Jia Y-L, Jiang Y-Q, Zhang Y-C. Mechanical properties and fatigue failure mechanisms of purely self-piercing riveted (SPR) and hybrid (SPR-bonded) joints under salt spray environment. *J Mater Res.* 2022;20:2501–17. <https://doi.org/10.1016/j.jmrt.2022.08.024>.
65. Yang B, Shan H, Liang Y, Ma Y, Niu S, Zhu X, et al. Effect of adhesive application on friction self-piercing riveting (F-SPR) process of AA7075-T6 aluminum alloy. *J Mater Process Technol.* 2022;299:117336. <https://doi.org/10.1016/j.jmatprotec.2021.117336>.
66. Liu Y, Zhuang W. Self-piercing riveted-bonded hybrid joining of carbon fibre reinforced polymers and aluminium alloy sheets. *Thin Walled Struct.* 2019;144:106340. <https://doi.org/10.1016/j.tws.2019.106340>.
67. Jiang H, Liao Y, Gao S, Li G, Cui J. Comparative study on joining quality of electromagnetic driven self-piercing riveting, adhesive and hybrid joints for Al/steel structure. *Thin Walled Struct.* 2021;164:107903. <https://doi.org/10.1016/j.tws.2021.107903>.
68. Alves LM, Dias EJ, Martins PAF. Joining sheet panels to thin-walled tubular profiles by tube end forming. *J Clean Prod.* 2011;19(6):712–9. <https://doi.org/10.1016/j.jclepro.2010.12.014>.
69. Alves L, Afonso R, Silva C, Martins P. Joining sandwich composite panels to tubes. *Proc Inst Mech Eng Part L J Mater Des Appl.* 2019;233(7):1472–81. <https://doi.org/10.1177/1464420718763463>.
70. Alves LM, Afonso RM, Silva CMA, Martins PAF. Boss forming of annular flanges in thin-walled tubes. *J Mater Process Technol.* 2017;250:182–9. <https://doi.org/10.1016/j.jmatprotec.2017.07.011>.
71. Alves LM, Silva CMA, Martins PAF. End-to-end joining of tubes by plastic instability. *J Mater Process Technol.* 2014;214(9):1954–61. <https://doi.org/10.1016/j.jmatprotec.2014.04.011>.
72. Alves LM, Afonso RM, Martins PAF. Self-pierce riveting of tubes to sheets. *Int J Adv Manuf Technol.* 2020;111(11):3351–60. <https://doi.org/10.1007/s00170-020-06347-x>.
73. Afonso RM, Alves LM, Martins PAF. Joining by boss forming of rods and tubes to sheets. *J Adv J Process.* 2020;1:100001. <https://doi.org/10.1016/j.jajp.2019.100001>.
74. Reichel A, Sampaio RFV, Pragana JPM, Bragança IMF, Silva CMA, Martins PAF. Form-fit joining of hybrid busbars using a flexible tool demonstrator. *Proc Inst Mech Eng Part L J Mater Des Appl.* 2021;236(6):1164–75. <https://doi.org/10.1177/14644207211060309>.
75. Pragana JPM, Baptista RJS, Bragança IMF, Silva CMA, Alves LM, Martins PAF. Manufacturing hybrid busbars through joining by forming. *J Mater Process Technol.* 2020;279:116574. <https://doi.org/10.1016/j.jmatprotec.2019.116574>.
76. Sampaio RFV, Pragana JPM, Bragança IMF, Silva CMA, Martins PAF. A self-clinching fastener for hidden lap joints. *CIRP J Manuf Sci Technol.* 2022;37:434–42. <https://doi.org/10.1016/j.cirpj.2022.02.022>.
77. Sampaio RFV, Pragana JPM, Clara RG, Bragança IMF, Silva CMA, Martins PAF. New self-clinching fasteners for electric conductive connections. *J Manuf Mater Process.* 2022;6(6):159.
78. Kasaei MM, da Silva LF. Joining sheets made from dissimilar materials by hole hemming. *Proc Inst Mech Eng Part L J Mater Des Appl.* 2022;236(6):1321–32. <https://doi.org/10.1177/14644207211072676>.
79. Lambiase F, Di Ilio A. Damage analysis in mechanical clinching: experimental and numerical study. *J Mater Process Technol.* 2016;230:109–20. <https://doi.org/10.1016/j.jmatprotec.2015.11.013>.
80. Ewenz L, Kuczyk M, Zimmermann M. Effect of the tool geometry on microstructure and geometrical features of clinched aluminum. *J Adv Join Process.* 2022;5:100091. <https://doi.org/10.1016/j.jajp.2021.100091>.
81. Kupfer R, Köhler D, Römisch D, Wituschek S, Ewenz L, Kalich J, et al. Clinching of aluminum materials—methods for the continuous characterization of process, microstructure and properties. *J Adv Join Process.* 2022;5:100108. <https://doi.org/10.1016/j.jajp.2022.100108>.
82. Alves LM, Afonso RM, Martins PAF. Double-sided self-pierce riveting of polymer sheets. *J Adv Join Process.* 2021;3:100051. <https://doi.org/10.1016/j.jajp.2021.100051>.
83. Schramm B, Harzheim S, Weiß D, Joy TD, Hofmann M, Mergheim J, et al. A review on the modeling of the clinching process chain—part III: operational phase. *J Adv Join Process.* 2022;6:100135. <https://doi.org/10.1016/j.jajp.2022.100135>.
84. Qin D, Chen C, Ouyang Y, Wu J, Zhang H. Finite element methods used in clinching process. *Int J Adv Manuf Technol.* 2021;116(9):2737–76. <https://doi.org/10.1007/s00170-021-07602-5>.
85. Alves LM, Moghadam M, Afonso RM, Nielsen CV, Martins PA. On the applicability limits of double-sided self-pierce riveting. *Proc Inst Mech Eng Part L J Mater Des Appl.* 2022;236(10):2027–36. <https://doi.org/10.1177/14644207221093627>.
86. Schramm B, Friedlein J, Gröger B, Bielak C, Bobbert M, Gude M, et al. A review on the modeling of the clinching process chain—part II: joining process. *J Adv Join Process.* 2022;6:100134. <https://doi.org/10.1016/j.jajp.2022.100134>.
87. Karathanasopoulos N, Pandya KS, Mohr D. Self-piercing riveting process: Prediction of joint characteristics through finite element and neural network modeling. *J Adv Join Process.* 2021;3:100040. <https://doi.org/10.1016/j.jajp.2020.100040>.
88. Karathanasopoulos N, Mohr D. Strength and failure of self-piercing riveted aluminum and steel sheet joints: multi-axial experiments and modeling. *J Adv Join Process.* 2022;5:100107. <https://doi.org/10.1016/j.jajp.2022.100107>.
89. Meng X, Huang Y, Cao J, Shen J, dos Santos JF. Recent progress on control strategies for inherent issues in friction stir welding. *Prog Mater Sci.* 2021;115:100706.
90. Ma Z, Feng A, Chen D, Shen J. Recent advances in friction stir welding/processing of aluminum alloys: microstructural evolution and mechanical properties. *Crit Rev Solid State Mater Sci.* 2018;43(4):269–333.
91. Bhardwaj N, Narayanan RG, Dixit U, Hashmi M. Recent developments in friction stir welding and resulting industrial practices. *Adv Mater Process Technol.* 2019;5(3):461–96.
92. Akbari M, Aliha M, Keshavarz S, Bonyadi A. Effect of tool parameters on mechanical properties, temperature, and force generation during FSW. *Proc Inst Mech Eng Part L J Mater Des Appl.* 2019;233(6):1033–43.
93. Beygi R, Kazeminezhad M, Mehrizi MZ, Loureiro A. Friction stir butt welding of Al–Cu bilayer laminated composites: analysis of force, torque, and temperature. *Int J Adv Manuf Technol.* 2017;88(1):393–400.
94. Sampaio RF, Pragana JP, Bragança IM, Silva CM, Martins PA. Thermo-electrical performance of hybrid busbars: an experimental and numerical investigation. *Proc Inst Mech Eng Part L J Mater Des Appl.* 2022;2022:14644207221102514.
95. Takeoka N, Tsuchida T, Matsuda T, Ogura T, Ohashi R, Hirose A. Analysis of mechanical properties of dissimilar material joint using scrubbing refill friction stir spot welding. *J Adv Join Process.* 2022;5:100112.
96. Fukada S, Ohashi R, Fujimoto M, Okada H. Refill friction stir spot welding of dissimilar materials consisting of A6061 and hot dip zinc-coated steel sheets. *Proceedings of the 1st international joint symposium on joining and welding*: Elsevier; 2013. p. 183–7.

97. Liu H, Hu Y, Wang H, Du S, Sekulic DP. Stationary shoulder supporting and tilting pin penetrating friction stir welding. *J Mater Process Technol.* 2018;255:596–604.
98. Davies P, Wynne B, Rainforth W, Thomas M, Threadgill P. Development of microstructure and crystallographic texture during stationary shoulder friction stir welding of Ti-6Al-4V. *Metall and Mater Trans A.* 2011;42(8):2278–89.
99. Gangwar K, Ramulu M. Friction stir welding of titanium alloys: a review. *Mater Des.* 2018;141:230–55.
100. Beygi R, Zarezadeh Mehrizi M, Akhavan-Safar A, Safaei S, Loureiro A, da Silva L. Design of friction stir welding for butt joining of aluminum to steel of dissimilar thickness: heat treatment and fracture behavior. *Int J Adv Manuf Technol.* 2021;112(7):1951–64.
101. Beygi R, Carbas R, Queiros A, Marques E, Shi R, da Silva L. Comparative study between stainless steel and carbon steel during dissimilar friction stir welding with aluminum: kinetics of Al-Fe intermetallic growth. *Met Mater Int.* 2022;28(8):1948–59.
102. You J, Zhao Y, Dong C, Miao S, Liu Z, Liu L, et al. Microstructural evolution and mechanical properties of the Al-Cu dissimilar joint enhanced by stationary-dynamic shoulder friction stir welding. *J Mater Process Technol.* 2022;300:117402.
103. Vicharapu B, Liu H, Fujii H, Narasaki K, Ma N, De A. Probing residual stresses in stationary shoulder friction stir welding process. *Int J Adv Manuf Technol.* 2020;106(5):1573–86.
104. Sundar AS, Adepu K, Mugada KK, Satyanarayana M. Effect of the static shoulder on microstructural, textural, and mechanical characteristics during friction stir welding of Al6061. *Proceedings of the institution of mechanical engineers part I-journal of materials-design and applications*; 2022.
105. Li X, Chen S, Yuan T, Jiang X, Han Y. Improving the properties of friction stir welded 2219-T87 aluminum alloy with GTA offset pre-heating. *J Manuf Process.* 2020;51:10–8.
106. Saha R, Biswas P. Current status and development of external energy-assisted friction stir welding processes: a review. *Weld World.* 2022;2022:1–33.
107. Çam G. Friction stir welded structural materials: beyond Al-alloys. *Int Mater Rev.* 2011;56(1):1–48.
108. Raturi M, Bhattacharya A. Microstructure and texture correlation of secondary heating assisted dissimilar friction stir welds of aluminum alloys. *Mater Sci Eng A.* 2021;825:141891.
109. Nath RK, Maji P, Barma JD. Development of a self-heated friction stir welding tool for welding of polypropylene sheets. *J Braz Soc Mech Sci Eng.* 2019;41(12):1–13.
110. Mahmoudiniya M, Kokabi AH, Goodarzi M, Kestens LA. The effect of improved cooling on the microstructure and mechanical properties of friction stir-welded advanced high-strength dual-phase steel. *Steel Res Int.* 2021;92(2):2000253.
111. Derazkola HA, Garcia E, Elyasi M. Underwater friction stir welding of PC: experimental study and thermo-mechanical modelling. *J Manuf Process.* 2021;65:161–73.
112. Zuiko IS, Mironov S, Betsofen S, Kaibyshev R. Suppression of abnormal grain growth in friction-stir welded Al-Cu-Mg alloy by lowering of welding temperature. *Scripta Mater.* 2021;196:113765.
113. Lezaack MB, Simar A. Avoiding abnormal grain growth in thick 7XXX aluminium alloy friction stir welds during T6 post heat treatments. *Mater Sci Eng A.* 2021;807:140901.
114. Rathinasuriyan C, Pavithra E, Sankar R, Kumar V. Current status and development of submerged friction stir welding: a review. *Int J Precis Eng Manuf Green Technol.* 2021;8(2):687–701.
115. Wahid MA, Khan ZA, Siddiquee AN, Shandley R, Sharma N. Analysis of process parameters effects on underwater friction stir welding of aluminum alloy 6082-T6. *Proc Inst Mech Eng Part B J Eng Manuf.* 2019;233(6):1700–10.
116. Patel V, De Backer J, Hindsefelt H, Igestrand M, Azimi S, Andersson J, et al. High-speed friction stir welding in light weight battery trays for the EV industry. *Sci Technol Weld Join.* 2022;27(4):250–5.
117. Mirabzadeh R, Parvaneh V, Ehsani A. Estimating and optimizing the flexural strength of bonding welded polypropylene sheets by friction-stir welding method. *Proc Inst Mech Eng Part L J Mater Des Appl.* 2021;235(1):73–86.
118. Huang Y, Meng X, Xie Y, Li J, Wan L. New technique of friction-based filling stacking joining for metal and polymer. *Compos B Eng.* 2019;163:217–23.
119. Reza-E-Rabby M, Ross K, Overman NR, Olszta MJ, McDonnell M, Whalen SA. Joining thick section aluminum to steel with suppressed FeAl intermetallic formation via friction stir dovetailing. *Scripta Mater.* 2018;148:63–7.
120. Momeni M, Guillot M. Development of friction stir welding technique at right angle (RAFSW) applied on butt joint of AA6061-T6 aluminum alloy. *Int J Adv Manuf Technol.* 2018;99(9):3077–89.
121. Imani Y, Guillot M. Tolerating for joint fit-up issues using welding parameters in friction stir welding of AA6061-T6 at right angle. *International congress of canadian society for mechanical engineering CSME, Canada*; 2014.
122. Sudhagar S, Sakthivel M, Ganeshkumar P. Monitoring of friction stir welding based on vision system coupled with machine learning algorithm. *Measurement.* 2019;144:135–43.
123. Murthy V, Ullegaddi K, Mahesh B, Rajaprakash B. Application of image processing and acoustic emission technique in monitoring of friction stir welding process. *Mater Today Proc.* 2017;4(8):9186–95.
124. Mishra D, Roy RB, Dutta S, Pal SK, Chakravarty D. A review on sensor based monitoring and control of friction stir welding process and a roadmap to Industry 4.0. *J Manuf Process.* 2018;36:373–97.
125. Roy RB, Ghosh A, Bhattacharyya S, Mahto RP, Kumari K, Pal SK, et al. Weld defect identification in friction stir welding through optimized wavelet transformation of signals and validation through X-ray micro-CT scan. *Int J Adv Manuf Technol.* 2018;99(1):623–33.
126. Mishra D, Gupta A, Raj P, Kumar A, Anwer S, Pal SK, et al. Real time monitoring and control of friction stir welding process using multiple sensors. *CIRP J Manuf Sci Technol.* 2020;30:1–11.
127. Chen G, Zhang S, Zhu Y, Yang C, Shi Q. Thermo-mechanical analysis of friction stir welding: a review on recent advances. *Acta Metall Sin (Engl Lett).* 2020;33(1):3–12.
128. Flint T, Francis J, Smith M. A semi-analytical solution for the transient temperature field generated by a volumetric heat source developed for the simulation of friction stir welding. *Int J Therm Sci.* 2019;138:586–95.
129. Bora B, Chattopadhyaya S, Kumar R. Development of mathematical model for friction stir welded joint using 'R' programming. *Mater Today Proc.* 2020;27:2142–6.
130. Beygi R, Marques E, da Silva LF. *Computational concepts in simulation of welding processes.* London: Springer; 2022.

131. Sarikavak Y. An advanced modelling to improve the prediction of thermal distribution in friction stir welding (FSW) for difficult to weld materials. *J Braz Soc Mech Sci Eng.* 2021;43(1):1–14.
132. Chu Q, Li W, Wu D, Liu X, Hao S, Zou Y, et al. In-depth understanding of material flow behavior and refinement mechanism during bobbin tool friction stir welding. *Int J Mach Tools Manuf.* 2021;171:103816.
133. Donea J, Huerta A, Ponthot JP, Rodríguez-Ferran A. Arbitrary Lagrangian–Eulerian methods. *Encyclopedia of computational mechanics*; 2004.
134. Ducobu F, Rivière-Lorphèvre E, Filippi E. Application of the coupled Eulerian–Lagrangian (CEL) method to the modeling of orthogonal cutting. *Eur J Mech A/Solids.* 2016;59:58–66.
135. Hannachi N, Khalfallah A, Leitão C, Rodrigues D. Thermo-mechanical modelling of the friction stir spot welding process: effect of the friction models on the heat generation mechanisms. *Proc Inst Mech Eng Part L J Mater Des Appl.* 2022;2022:14644207211070965.
136. Akbari M, Asadi P. Dissimilar friction stir lap welding of aluminum to brass: modeling of material mixing using coupled Eulerian–Lagrangian method with experimental verifications. *Proc Inst Mech Eng Part L J Mater Des Appl.* 2020;234(8):1117–28.
137. Yu Z, Zhang W, Choo H, Feng Z. Transient heat and material flow modeling of friction stir processing of magnesium alloy using threaded tool. *Metall Mater Trans A.* 2012;43(2):724–37.
138. Wang X, Gao Y, Liu X, McDonnell M, Feng Z. Tool-workpiece stick-slip conditions and their effects on torque and heat generation rate in the friction stir welding. *Acta Mater.* 2021;213:116969.
139. Zhao C, Liu X. An alternative pressure-dependent velocity boundary condition for modeling self-reacting friction stir welding. *Int J Adv Manuf Technol.* 2021;117(5):1601–13.
140. Fraser K, St-Georges L, Kiss L. Numerical simulation of bobbin tool friction stir welding. *Proceedings of the 10th international friction stir welding symposium*; 2014.
141. Eivani A, Vafaenezhad H, Jafarian H, Zhou J. A novel approach to determine residual stress field during FSW of AZ91 Mg alloy using combined smoothed particle hydrodynamics/neuro-fuzzy computations and ultrasonic testing. *J Magn Alloys.* 2021;9(4):1304–28.
142. Muhammad NA, Wu C. Evaluation of capabilities of ultrasonic vibration on the surface, electrical and mechanical behaviours of aluminium to copper dissimilar friction stir welds. *Int J Mech Sci.* 2020;183:105784.
143. Le Jolu T, Morgeneyer TF, Denquin A, Sennour M, Laurent A, Besson J, et al. Microstructural characterization of internal welding defects and their effect on the tensile behavior of FSW joints of AA2198 Al–Cu–Li alloy. *Metall Mater Trans A.* 2014;45(12):5531–44.
144. Aghabeigi M, Hassanifard S, Hashemi SM. Evaluation of different strain-based damage criteria for predicting the fatigue life of friction stir spot-welded joints under multi-axial loading conditions. *Proc Inst Mech Eng Part L J Mater Des Appl.* 2020;234(1):156–66.
145. Beygi R, Pouraliakbar H, Torabi K, Fallah V, Kim S, Shi R, et al. The inhibitory effect of stir zone liquefaction and eutectic-phase formation on the growth of γ/β intermetallics during dissimilar FSW of Al/Mg alloys. *J Manuf Process.* 2021;70:152–62.
146. Wang F, Li W, Shen J, Wen Q, Dos Santos J. Improving weld formability by a novel dual-rotation bobbin tool friction stir welding. *J Mater Sci Technol.* 2018;34(1):135–9.
147. Wang F, Li W, Shen J, Hu S, Dos Santos J. Effect of tool rotational speed on the microstructure and mechanical properties of bobbin tool friction stir welding of Al–Li alloy. *Mater Des.* 2015;86:933–40.
148. Zeng S, Chen G, Dinaharan I, Liu Q, Zhang S, Sahu PK, et al. Microstructure and tensile strength of AA6082 T-joints by corner stationary shoulder friction stir welding: effect of tool rotation speed. *J Mater Eng Perform.* 2020;29(11):7094–103.
149. Liu H, Hou J, Guo H. Effect of welding speed on microstructure and mechanical properties of self-reacting friction stir welded 6061-T6 aluminum alloy. *Mater Des.* 2013;50:872–8.
150. Beygi R, Kazeminezhad M, Kokabi A, Loureiro A. Friction stir welding of Al–Cu bilayer sheet by tapered threaded pin: microstructure, material flow, and fracture behavior. *Metall Mater Trans A.* 2015;46(6):2544–53.
151. Beygi R, Akhavan-Safar A, Carbas R, Barbosa A, Marques E, da Silva L. Utilizing a ductile damage criterion for fracture analysis of a dissimilar aluminum/steel joint made by friction stir welding. *Eng Fract Mech.* 2022;274:108775.
152. Kar A, Yadav D, Suwas S, Kailas SV. Role of plastic deformation mechanisms during the microstructural evolution and intermetallics formation in dissimilar friction stir weld. *Mater Charact.* 2020;164:110371.
153. Xu W, Luo Y, Fu M. Microstructure evolution in the conventional single side and bobbin tool friction stir welding of thick rolled 7085-T7452 aluminum alloy. *Mater Charact.* 2018;138:48–55.
154. Liu X, Sun Y, Nagira T, Ushioda K, Fujii H. Strain rate dependent micro-texture evolution in friction stir welding of copper. *Materialia.* 2019;6:100302.
155. Imam M, Sun Y, Fujii H, Ma N, Tsutsumi S, Ahmed S, et al. Deformation characteristics and microstructural evolution in friction stir welding of thick 5083 aluminum alloy. *Int J Adv Manuf Technol.* 2018;99(1):663–81.
156. Li G, Zhou L, Luo S, Dong F, Guo N. Microstructure and mechanical properties of bobbin tool friction stir welded ZK60 magnesium alloy. *Mater Sci Eng A.* 2020;776:138953.
157. Zhang J, Huang Y, Xiang J, Huang G, Chen X, Zhou H, et al. Characterization of newly developed friction stir-arc welding method for AM60/AZ31 dissimilar Mg alloy. *Mater Sci Eng A.* 2021;800:140320.

Publisher's Note Springer Nature remains neutral with regard to jurisdictional claims in published maps and institutional affiliations.